A reply to the review comments for

Cloud response to co-condensation of water and organic vapors over the boreal forest

Liine Heikkinen[1,2], Daniel G. Partridge[3], Sara Blichner[1,2], Wei Huang[4], Rahul Ranjan[1,2], Paul Bowen[3], Emanuele Tovazzi[3], Tuukka Petäjä[4], Claudia Mohr[1,2], and Ilona Riipinen[1,2]

[1]Department of Environmental Science (ACES), Stockholm University, Stockholm, Sweden
[2]Bolin Centre for Climate Research, Stockholm University, Stockholm, Sweden
[3]Department of Mathematics and Statistics, Faculty of Environment, Science and Economy, University of Exeter, Exeter, United Kingdom
[4]Institute for Atmospheric and Earth System Research (INAR) / Physics, University of Helsinki, Helsinki, Finland

Correspondence to: Liine Heikkinen (liine.heikkinen@aces.su.se) and Ilona Riipinen (ilona.riipinen@aces.su.se)

General information

We thank both reviewers for their detailed reviews on out manuscript. This document contains point-by-point responses to the questions and issues raised by the reviewers. As you may have noticed, it has taken us some time to finish the review response. This is because we chose to re-run all the simulations with a new version of the model. We thank the editor for their patience and giving us the extra time. While reworking the whole paper, we also caught few bugs and problems present in the previous manuscript version. In this section, we present three main changes in the manuscript that were not requested by the reviewers. Other smaller adjustments are visible in the revised manuscript version.

1. The model version for CPM simulations is changed since the last manuscript version from ICPM-UFO to **PARSEC-UFO.** PARSEC is build based on ICPM, and the agreement between the two models is excellent.
   - **Consequences:**
     - The model runs much faster, and the model version will eventually be released to the public.
   - **Manuscript edits:**
     - Paul Bowen has been added as a co-author due to his authorship in the PARSEC-UFO model and valuable simulation and analysis support.
     - ICPM changed to PARSEC-UFO throughout the manuscript
     - All tables and figures have been reconstructed (see the manuscript)

2. ***The $log_{10}C^*$ for the CJ simulations had wrongly assigned values*** in the previous manuscript version (they were equal to the $log_{10}C^*$ describing F-distribution i.e., -4:7 rather than -8:3). This led to an overestimation of the gas phase concentrations of organic vapors and thereby higher ΔCDNC were modelled due to co-condensation. The new manuscript version contains PARSEC-UFO simulations with the correct volatility axis.

   - **Consequences:**

- **▪ ΔCDNC due to co-condensation, when applying the CJ volatility distributions, are insignificant on average.** As these numbers are very different to those obtained in Topping et al. (2013), **we show that we can reproduce the Topping et al. (2013) results with PARSEC-UFO**. Furthermore, we conclude that the PARSEC-UFO initialization temperature, which controls the initial volatility distribution *x*-axis, can greatly influence the amount of organic vapor available for co-condensation. Under the PARSEC-UFO initialization temperature, the CJ yields on average only 0.1 µg m^{-3} of organic vapor available for co-condensation after PARSEC-UFO initialization, while in the case of the F distribution the organic vapor mass concentration is twenty times higher.

- **Manuscript edits:**

L621–L642:

"Besides updraft velocity, also PARSEC-UFO initialization temperature affects the modeled ΔCDNC. This can be seen when the effect of the volatility distribution upgrade (from CJ to F) on the modelled ΔCDNC is investigated. For this purpose, an additional set of PARSEC-UFO simulations using the CJ volatility distribution are performed. Perhaps surprisingly, the CDNC enhancements due to co-condensation attained with the CJ volatility distribution are negligible (median ΔCDNC is 0; Fig. S.7) and therefore strikingly different from those presented in Topping et al. (2013). It is discovered here that the large difference in the modeled ΔCDNC between the F and CJ simulations arises from the low amount of organic vapor available for condensation ($\sum C_g^{INIT}$ is only 0.10 µg m^{-3} in CJ simulations while in the F simulations it is 2.05 µg m^{-3}), which in turn results from the low PARSEC-UFO initialization temperature attained from the radio soundings (Sect. 2.2). If the initialization temperatures were higher, more organic vapor would remain in the gas phase after PARSEC-UFO initialization, and larger ΔCDNC could be modeled. The simulations performed in Topping et al. (2013) were initialized at 298 K, which explains why they report significant CDNC enhancements due to co-condensation using a similar CJ volatility distribution as used here. We can reproduce the Topping et al. (2013) findings when increasing the initialization temperature with PARSEC-UFO (see Fig. S.8) and also demonstrate that by decreasing the initialization temperature from 298 to 280 K (the BAECC median temperature), the ΔCDNC modeled by Topping et al. (2013) should also be negligible (Fig. S.8). These findings emphasize the critical role of the initialization temperature (and assumptions made on equilibrium upon model initialization) that impacts the amount of organic vapor present in the gas phase prior to the air parcel's ascent. Additionally, the result suggests high importance of organic vapors with saturation vapor concentrations exceeding $log_{10}C* = 3$ (under 298 K) for co-condensation. If one were to utilize CJ

distributions in future co-condensation work, one could consider multiplying the highest volatility bins e.g., with a carefully selected constant. Similar approaches have been used previously when modeling SOA formation from IVOCs (Lu et al., 2018)."

Supplementary Figure 7:
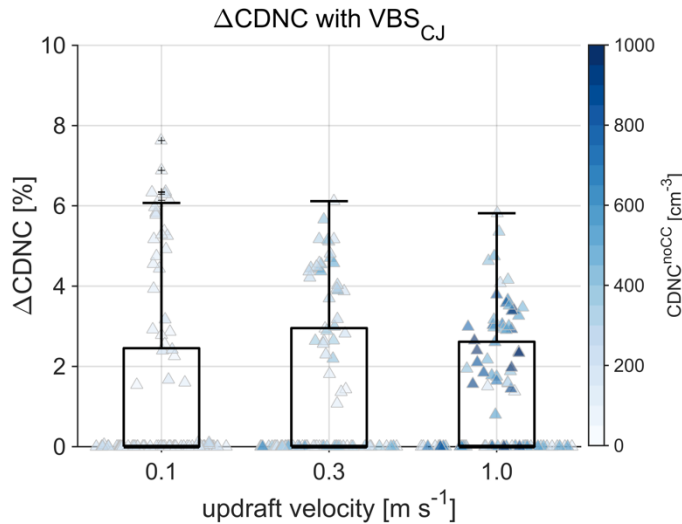
*"**Figure S.7** Box plots showing the predicted ΔCDNC (using CJ volatility distributions) due to co-condensation in the three different modelling scenarios (0.1, 0.3 and 1.0 m s⁻¹ updrafts). The colored markers represent CDNC (without accounting for co-condensation) in form of a swarmplot."*

Supplementary Figure 8:
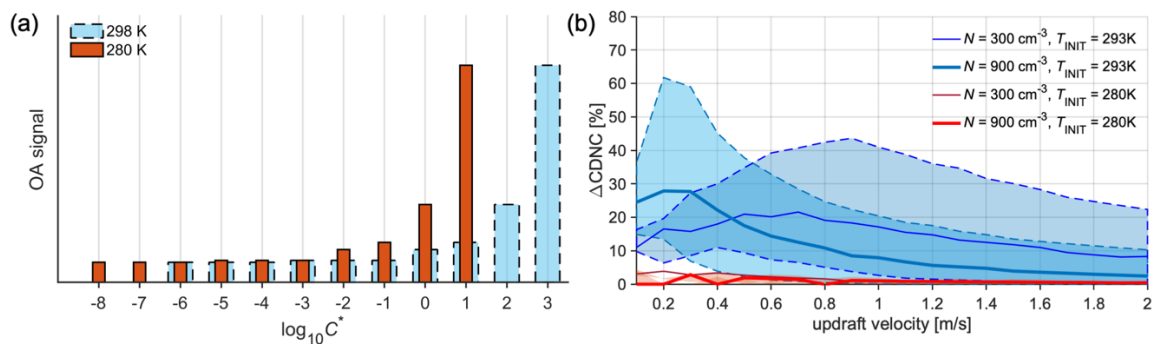
*"**Figure S.8** (a) The volatility basis set shown in Topping et al. (2013) under their reported initialization temperature (light blue) and under the mean BAECC initialization temperature (in red). The $log_{10}C^*$ axis is shifted according using Eq. (13), found in the main text of the paper. (b) The impact of initialization temperature on Figure 3 in Topping et al. (2013) using an initialization RH of 80%. High CDNC enhancements due to co-condensation using the blue volatility distribution is modeled for clean and polluted cases, and agreement with Topping et al. (2013) is found. When utilizing the temperature-adjusted volatility distribution, and initialization temperature of 280 K, and initialization RH of 80% no significant CDNC enhancements are modeled."*

Responses to review comments

In the following, the reviewer comments are written in **red** and our responses in **black**.

Reviewer #1

The manuscript describes modelling experiments regarding co-condensation of organic vapour and water in a rising air parcel. The main improvement compared to previous work is better quantification of the more volatile vapours using the FIGAERO-I-CIMS observations. The topic of the paper is interesting, as co-condensation could potentially have significant impact on cloud droplet activation but this effect is currently ignored in majority of models. The paper is generally well written and detailed.

We thank the reviewer for this encouraging statement and the interesting and important comments, which we have addressed below.

Comments:

1. **In the introduction the authors should briefly explain how co-condensation differs from separately simulating condensation of water (taking into account hygroscopicity of the aerosol) and organic vapours (e.g. original VBS that doesn't account for water in the particle), as it is presently commonly done in models.**

   Reply: Thank you for requesting this. We have clarified the point.

   Manuscript edits:

   ### L69–L94:

   "Numerous studies have been carried out to understand the role of condensable organic vapors in SOA formation (e.g., Hallquist et al., 2009; Shrivastava et al., 2017) and hence the concentrations of CCN (i.e. particles of at least 50–100 nm in diameter for the water vapor supersaturations typical of the boreal environments; Cerully et al., 2011; Sihto et al., 2011; Paramonov et al., 2013; Hong et al., 2014; Paramonov et al., 2015). The yields of volatile, intermediate-volatility or semi-volatile organic compounds (VOCs, IVOCs, or SVOCs) from monoterpene oxidation, such as those of pinonaldehyde, formic acid, or acetic acid, are generally much higher than those of the readily condensable lower-volatility vapors (low-volatility organic compounds, LVOCs and extremely low volatility organic compounds, ELVOCs), but they are typically not considered directly important for SOA or CCN formation. The above-mentioned volatility classes are determined based on the volatilities of individual compounds binned into a volatility basis set (VBS; Donahue et al., 2006): VOCs have a saturation vapor concentration (C^*; given in units of $\mu g\ m^{-3}$ throughout the paper) of at least $10^7\ \mu g\ m^{-3}$, IVOCs are distributed in the C^* range of $[10^3, 10^6]\ \mu g\ m^{-3}$, SVOCs of $[1, 100]$, LVOCs of $[10^{-3}, 10^{-1}]$ and ELVOCs have a C^* below $10^{-4}\ \mu g\ m^{-3}$ (e.g., Donahue et al., 2011). While VOCs, IVOCs, and some SVOCs are unlikely to produce significant concentrations of SOA at ground level without additional oxidation steps or multiphase chemistry, some of them can condense at

higher altitudes if transported aloft (e.g., Murphy et al., 2015). In addition, aerosol liquid water plays a key role in determining the amount of SVOCs and IVOCs in the condensed phase. Liquid water acts as an absorptive medium, and a higher liquid water content can enable a higher quantity of organic vapors to partition into the condensed phase. However, the role of water in determining partitioning coefficients is often neglected when absorptive partitioning theory (Pankow et al., 2001) is applied. Barley et al. (2009) demonstrated that the inclusion of water, when predicting absorptive partitioning using Raoult's law, could lead to evident increases in organic aerosol (OA) mass concentrations under atmospherically relevant OA loadings. Later work by Topping and McFiggans (2012) showed how under a decreasing temperature trend, the concentration of aerosol liquid water increases making the solution particle more dilute enabling enhanced dynamic partitioning of organic vapors (together with water vapor). This work focuses on the dynamic SVOC and IVOC condensation together with water vapor (co-condensation) in rising and cooling air motions, and the effects co-condensation poses on cloud microphysics."

2. line 86: "the cooling of the rising air triggers also their condensation" – this gives the impression that the condensation of the higher volatility vapours is purely due to lower temperature, while actually the main driver seems to be the aerosol water content. Please restate.

Reply: Thank you for requesting this. We have clarified the point.

Manuscript edits:

L95–L107:

"Warm (liquid) clouds can form when air rises and cools, eventually leading to the air being supersaturated with water vapor. The excess water vapor condenses onto aerosol particles, rapidly growing them into cloud droplets. While water represents the most abundant vapor in the atmosphere, also other trace species can influence the cloud droplet activation process as the cooling of the rising air triggers also their condensation. The partitioning of these other vapors is partially driven by the decrease in temperature itself, which makes the species less volatile, but more important it is the increase in aerosol liquid water, and the dilution of the aerosol solution that enables them to partition to the liquid phase (Topping and McFiggans, 2012). As the trace vapors condense in the rising air under sub-saturated conditions, the molar fraction of water in the swelling aerosol particles increases slower than in the absence of this co-condensation process, which in turn leads to the condensation of additional water by the time the air parcel reaches lifting condensation level. The co-condensation of water with other trace vapors eventually leads to a reduction in critical supersaturation (s^*) required for droplet activation of the particles due to an increased amount of organic solute (Topping and McFiggans, 2012), as described by Köhler theory (Köhler, 1936)."

The authors should carefully check all their formulas. For example: Formula (5), line 184 : "ρ_a is the density of the particle dry mass" –shouldn't this be air density, as n_{ij} is probably per cubic meter? Formula (14): The condensation of organic species seems to depend only on water density and molar mass, of which the density seems to cancel out?

Reply: We thank the reviewer for also reviewing the formulae. We have carefully checked them, and adjusted the manuscript. Also Eq. (10) required improvement.

Manuscript edits:

L208–L211:

"the liquid water mixing ratio (x_L) is calculated as a sum of the liquid water mixing ratio across all the 400 size bins (index i) for each assigned mode composition (index j):

$$\Delta x_L = \frac{4\pi\rho_w}{3\rho_a} \sum_{i=1}^{n_a} \sum_{j=1}^{n_b} n_{ij}\left(r_{ij}^3 - r_{ij,\,\text{dry}}^3\right),\tag{5}$$

where ρ_w is density of water, **ρ_a is the density of dry air**, n_{ij} is the number of particles within size bin i and composition j, and finally r_{ij} and $r_{ij,\,dry}$ are the wet and dry radii of the particles, respectively."

L237–244:

"The condensation/evaporation equation for organic species is described in the same manner as in Topping et al. (2013) and as shown for water vapor in Eq (6):

$$\frac{\mathrm{d}m_q}{\mathrm{d}t} = \frac{4\pi\,\rho_w\,r\,\text{DIFF}_g^*\left(S_q - S_{\text{eq},q}\right)e_{s,q}}{\dfrac{\text{DIFF}_g^*\Delta H_{\text{vap},q}\,S_{\text{eq},q}\,e_{s,q}\,\rho_q}{\lambda\,T}\left(\dfrac{\Delta H_{\text{vap},q}}{R_{v,q}\,T} - 1\right) + \rho_q\,R_{v,q}\,T}\tag{11}$$

where DIFF_g^* is the gas phase diffusivity (see details in Topping et al., 2013 supplementary information), and λ is the heat conductivity of air. Both DIFF_g^* and λ are corrected for the transition regime of condensation. $\Delta H_{vap,q}$ is the enthalpy of vaporization, $e_{s,q}$ the saturation vapor pressure, $S_{eq,\,q}$ the equilibrium saturation ratio and ρ_q the density of organic species in the qth volatility bin."

L226–232:

"

$$B = \frac{\phi_S\,M_w\,\varepsilon_V\,\rho_s\,\nu}{M_s\,\rho_w}\tag{10}$$

.

A and B in Eqs. (9) and (10) are the Köhler coefficients, where M_w is the molecular weight of water (g mol⁻¹), M_s refers to the molar mass of the soluble fraction, ρ_w is the density of water (g m⁻³), ϕ_s is the osmotic coefficient of salt in the solution ($\phi_s \approx 1$ in ideal solutions), ν is the dissociation constant, and ρ_s and ε_V are the density and the volume fraction of the soluble mass in the aerosol particle, respectively. The dissociation constant is calculated as $\nu = (\sum_i c_i^+ + \sum_j c_j^-)/\sum_{ij} c_{ij}$, where, c_i^+ and c_j^- are the concentrations of positive and negative ions and c_{ij} is the concentration (mol L⁻¹) of the electrolytes in solution. For detailed descriptions of the B term, the reader is directed to Roelofs (1992)."

3. **It is unclear from the description of the CPM what assumptions have been made about the hygroscopicity of the condensing organics. What value of hygroscopicity parameter for the SOA would these assumptions lead to? How does it compare with other modelling studies or observations?**

Reply: The description of the Köhler *B*-term has been improved (see previous point), which hopefully helps in understanding how hygroscopicity is treated. The κ for organics is the maximum κ organics can attain (organics do not dissociate). It and can be calculated as

$$\kappa_{\text{org, max}} = \frac{M_w}{M_{\text{org}}} \frac{\rho_{\text{org}}}{\rho_w},$$

where M_w is the molar mass of water, M_{org} the molar mass of organics, ρ_{org} the density of organics and ρ_w the density of water (Petters and Kreidenweis, 2008; Riipinen et al., 2015). For the simulations shown here, M_{org} is 0.2 kg mol⁻¹ and ρ_{org} is 1500 kg m⁻³ throughout the volatility bins and therefore, $\kappa_{\text{org, max}} = 0.135$ (modeling studies typically assume that $\kappa = 0.1$ for organics). κ-values have been previously determined for SMEAR II organic aerosol (e.g., Jimenez et al., 2009; Paramonov et al., 2013). SV-OOA was determined to have a κ between 0 and 0.02, and LV-OOA between 0.18 and 0.22 (Jimenez et al., 2009). The PARSEC-UFO simulations are performed during the day, when LV-OOA dominates the OA (roughly 75% of OA is LV-OOA). Sihto et al. (2011) estimate that $\kappa = 0.18$ is representative of SMEAR II aerosol as it yields the best closure between measured and modeled CCN number concentrations. The hygroscopicity of the SMEAR II aerosol within PARSEC-UFO simulations exceeds this number (median 0.32 in our simulations), because κ for ammonium sulfate (κ_{AS}) in the ideal solution is 0.72. When κ_{AS} are derived from experimental data, the values are lower (e.g., Schmale et al., 2018). A higher hygroscopicity for ammonium sulfate can influence the amount of organic vapor available for co-condensation, because of the higher aerosol liquid water content during model initialization that drives the organic vapor partitioning. We have added the κ values for ammonium sulfate and organics in the manuscript, where the PARSEC initialization is discussed.

Manuscript edits:

L290–301:

"Each modelled scenario has log-normal parameters describing a bimodal aerosol size distribution form BAECC measurements and the organic mass fraction from ACSM measurements (Sect. 2.3). The rest of the mass is assumed to be ammonium sulfate, which is generally a good approximation for SMEAR II (Heikkinen et al., 2020). For the simulations performed here, BC is not included given its small (about <5%) contribution to aerosol mass from late spring to summer (Luoma, 2021). While PARSEC-UFO does not utilize κ-Köhler theory (Petters and Kreidenweis, 2008), it might be useful to know that the assumed hygroscopicity, if translated to the hygroscopicity parameter κ, would be 0.14 and 0.72 for organics and ammonium sulfate, respectively (ideal solution; median $\kappa_{tot} \approx 0.32$). The assumed overall hygroscopicity is therefore likely to be overestimated, and it would exceed κ determined for SMEAR II experimentally in previous studies (e.g., Sihto et al., 2011 suggest $\kappa = 0.18$). Due to the likely overestimation of aerosol liquid water at initial conditions, it is also likely that the amount of organic vapor available for co-condensation after PARSEC-UFO initialization is underestimated."

4. How does UKESM simulate biogenic SOA and its precursors?

Reply: Information added to Sect. 2.5.

Manuscript edits:

L519–L521:

"UKESM1 uses a 26% SOA yield from monoterpenes, the emissions of which are from The Model of Emissions of Gases and Aerosols from Nature (MEGAN) version 2.1 (Guenther et al., 1995) ."

The authors convincingly show that new particle formation is an important factor for creating the suitable particle size distributions for co-condensation to affect the CDNC. However, boundary layer new particle formation is not included in UKESM simulations and the simulated size distributions are shown to be quite different from the ones observed in Hyytiälä. I am not sure if there is any value in showing these results in this already long paper.

Reply: It is correct that the results from the UKESM1 exercise (Sect. 3.5) are perhaps not extremely indicative of the effects co-condensation could have on droplet number in reality. However, as there is currently scientific interest to develop parameterization schemes for co-condensation and implementing those in GCMs, we believe that it is important to show also the limitations the ESM size distribution shapes can have for realistically capturing the effects co-condensation may play. It is therefore, we have formulated the text so that it says "how often does UKESM1 *experience* suitable size distributions" and the answer is: not often. However, we agree that this wording was not present in the abstract or conclusions. This finding (or the discrepancy between modeled and observed PNSD) hopefully motivates the ESM community to further work on implementing different NPF parameterization schemes and improving aerosol size distribution dynamics within the models in addition to

studying the benefits e.g., in using modal or sectional size distribution schemes in these models. We have clarified these important points, and hope the manuscript edits shown below also demonstrate the value of adding the UKESM1 results in the paper.

Manuscript edits:
L32–L38:

"Five years of UK Earth System Model (UKESM1) simulations are further used to evaluate the frequencies to which such distributions are experienced by an Earth System Model over the whole boreal biome. The frequencies are substantially lower than those observed at the boreal forest measurement site (<6% of the time) and the positive values, peaking in spring, are modeled only over Fennoscandia and western parts of Siberia. Overall, the similarities in the size distributions between observed and modeled (UKESM1) are limited, which would limit the ability of this model, or any model with a similar aerosol representation, to project the climate-relevance of co-condensation."

L891–904:

"Further on, UKESM1 simulations (years 2009–2013) are utilized to investigate the potential impact of including the process of co-condensation on droplet formation in this model over the whole boreal biome using the criteria developed from the SMEAR II case to identify most susceptible PNSD conditions. Overall, the UKESM1 PNSD are different from those observed at SMEAR II even when the strict criteria are used to select the ideal PNSD for co-condensation driven enhancements in CDNC. This discrepancy can arise from multiple causes such as the lack of critical aerosol processes (boundary layer new particle formation), but it can also be a common ESM feature arising from the modal representation of PNSD. Nonetheless, aside from two hotspots (one near the Rocky Mountains in North America, one over northern Kazakhstan, which are not analyzed further), the presence of suitable PNSD, as experienced by UKESM1, is most frequent over Fennoscandia and western parts of Siberia in spring, yet the frequencies at which those PNSD are modelled remained much lower than those obtained from the long-term SMEAR II PNSD measurements (2–6% in UKESM1). Perhaps surprisingly, suitable PNSD are never modeled over most of Siberia, suggesting that for the model configuration of UKESM1 used in this study, the process of co-condensation would not be expected to have an influence on droplet formation in this area. This is due to the low concentration of ultrafine particle particles modeled in the area. "

L905–914:

"In summary, these results highlight the potential significance of co-condensation in pristine boreal environments with a nascent ultrafine particle mode present. Such conditions are met over

Fennoscandia and Western parts of Siberia in Spring and to a lesser extent in the Fall, when NPF takes place. For future modelling purposes, it is vital to stress the importance of the accurate representation of PNSD for capturing the role of co-condensation of organics on CDNC enhancements, including appropriate description of boundary layer NPF. Because the modelled CDNC enhancements are so significant, further research focus especially regarding observations of the co-condensation should be targeted in the future to motive future assessments of co-condensation-driven radiative forcing. Perhaps this work inspires aircraft measurements (of the relevant parameters discussed in this paper) to take place over the Fennoscandia in the future to finally narrow down the importance of co-condensation for the accurate representation of CDNC in GCMs."*

Lines 493-501: Topping et al. (2013) found very significant reduction in condensation of their highest volatility bin. Taking into account that more volatile species are less soluble, the reduction should be even larger for the higher volatility bins of this study. Given that most of the condensed mass seems to come from bins where $\log_{10}C^* >= 3$, how large are the authors expecting the ideality related overestimations to be?

Reply: We thank the reviewer for this suggestion. We have performed a set of simulations with different mass accommodation coefficients for organics (α_{org}) to probe the effects of ideality on ΔCDNC. The results indicate that if the modeled ΔCDNC are particularly large, small reductions in α_{org} can result in large reductions in the projected cloud response. However, if looking into simulations with ΔCDNC close or below the BAECC median, then α_{org} reduction causes a noticeable change in ΔCDNC only if α_{org} < ~0.4. It is evident that the selection of the initial relative humidity or temperature (as shown in Fig. S.8) play a more important role in affecting ΔCDNC than α_{org}. We have added a small appendix to the manuscript discussing these points. This includes also a small demonstration of the ΔCDNC sensitivity to the selection of ΔH_{VAP}.

Manuscript edits:

Appendix A

The effect of the initialization relative humidity, organic mass accommodation coefficient and vaporization enthalpy on the modelled CDNC enhancements due to co-condensation are investigated for three individual simulations. The three simulations were selected as they are representative of low, median and high ΔCDNC simulated during BAECC (simulation IDs #13, #55 and #95, respectively; Table S.1).

The initialization RH affects the availability of organic vapor for co-condensation: when PARSEC-UFO is initialized under high RH (~>95%), most organic vapor is scavenged at initial conditions causing negligible enhancements in CDNC. On the other hand, if the initialization RH is lower (<90%), less organic vapor is scavenged at initial conditions, and the modeled ΔCDNC are greater (Fig. A.1). By varying α_{org}, the effect of the assumption of ideality has on the projected CDNC

enhancements is probed. For simplicity, the mass accommodation coefficient for organics (α_{org}) is set to be constant across the volatility bins. By reducing α_{org} from 1 to 0.8, the condensation of organics reduces. However, this impacts CDNC only in the simulation ID #95 (Fig. A.2; CDNC reduces from ~62% to 55%), i.e., simulation with the highest ΔCDNC. When $\alpha_{org} < 0.4$, also the simulation ID #55 shows a reduction in the modeled ΔCDNC as it drops from ~22% to ~15%. The selection of the enthalpy of vaporization for organics does not affect ΔCDNC (Fig. A.3). Over all, the initial relative humidity plays the most critical role out of the three parameters considered here (RH, α_{org} and ΔH_{VAP}), on the modelled ΔCDNC.
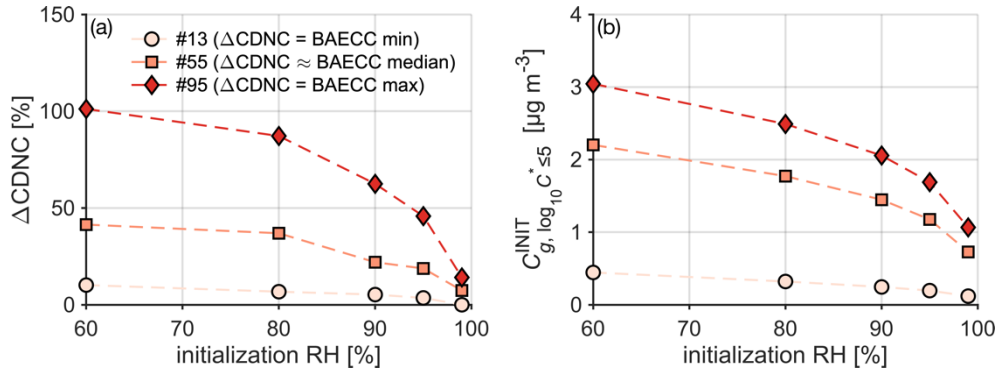
Figure A.1 The modelled CDNC enhancements as function of initialization RH ranging from 60% to 99% (indicated with different colors) for each simulation ID are shown, respectively. The initialization temperature and pressure are fixed to values shown in Table S.1. and only the volatility bins $log_{10}C^* \leq 5$ are included, which is motivated e.g., by Fig. 4. The simulations are performed with an updraft velocity of 0.3 m s^{-1}. The markers with the lightest color refer to the BAECC simulation, where co-condensation influenced ΔCDNC negligibly (ID #13, ΔCDNC = 3%), the orange markers to the BAECC median ΔCDNC (ID #55), and the red markers represent a simulation, where the modelled ΔCDNC was greatest (ID #95, ΔCDNC = 75%).
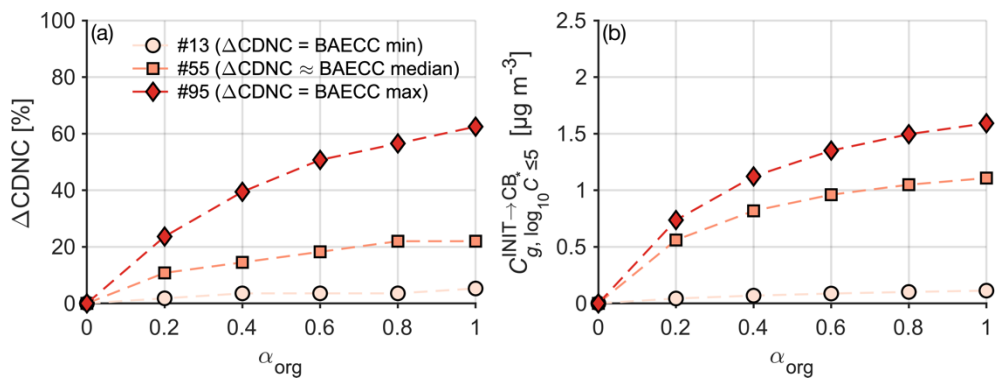
Figure A.2 The modelled CDNC enhancements as function of mass accommodation coefficient for organics (α_{org}) ranging from zero to one. The colorings and presented simulations are same as in Fig. A.1.
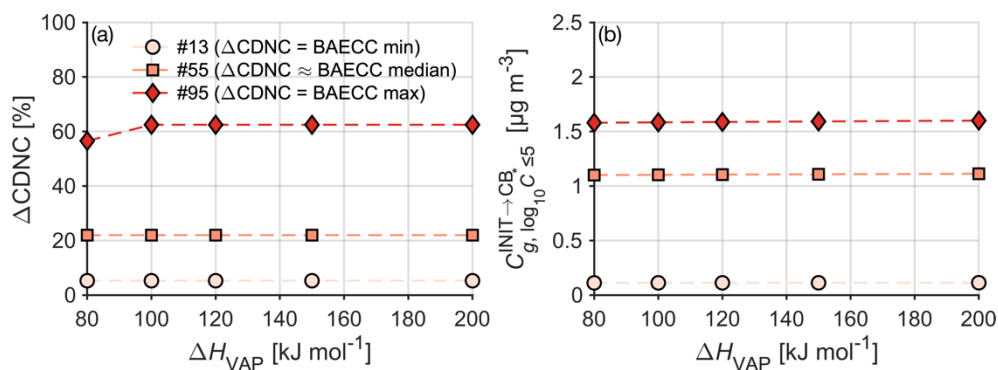
Figure A.3 *The modelled CDNC enhancements as function of vaporization enthalpy for organics (ΔH_VAP) ranging from zero to one. The colorings and presented simulations are same as in Fig. A.1.*

L550–L564:

"The exact numbers presented here should, however, be assessed with caution as an ideal liquid phase, as well as partitioning being determined by mole fractions of water-soluble organics are assumed (Sect. 2.1.1). Topping et al. (2013) looked into the assumption of ideality in their supplementary material. They found it to enhance the amount of modelled organic condensate as compared to a non-ideal case. However, their simulations exploring non-ideality with organic activity coefficients predicted with the UNIFAC method (UNIQUAC Functional-group Activity Coefficients; Fredenslund et al., 1975) still led to significant amounts of condensed organic mass. The impact of the ideality assumption was shown to be most significant in their highest volatility bin ($C^* = 1000\ \mu g\ m^{-3}$). Activity coefficients (and solubilities) of organics should in the future be better constrained to assess the impact on volatility bins of $\log_{10}C^* > 3$, which was not explored in Topping et al. (2013). As discussed in the Topping et al. (2013) supplementary information, it is likely that solubility decreases towards the higher volatility bins. Here, a simple assessment of the assumption of ideality (Appendix A, Fig. A.2b) suggests that the gained organic soluble mass reduces only when the overall mass accommodation coefficient for organics is less than 0.4. This would mean that the organic condensation shown here could be taken as the upper limit, however the equilibrium assumption at model initialization still limits the amount of organic vapor available for co-condensation (Sect. 2.2 and 3.3)."

L643–L658:

"As the results from Fig. 4 underline the time-dependence of co-condensation (Sect. 3.1), it is worth remembering that the PARSEC-UFO initialization RH is set to 90% where equilibrium conditions are assumed (see Sect. 2.4). Therefore, the kinetic effects play a role only from 90% to 100% RH. Importantly, if the initial RH was set to a lower value, more time would be available for co-condensation before reaching CB, and if the initial RH was set to a higher value, less time would be available. On the other hand, due to the assumption of initial equilibrium conditions, a lower initial

RH also ensures a higher organic vapor concentration available for co-condensation, and a higher initial RH reduces the organic vapor availability. Together with initial temperature, the initial RH strongly control the amount of organic vapor available for co-condensation (Appendix A, Fig. A.1, Fig. S.3) and thereby the amount of soluble organic mass yielded by the time the air parcel reaches cloud base. While the decision of maintaining a fixed initial RH for the different simulations is proven useful for this study as it eases the data interpretation process, it should be acknowledged that the initial RH could be better constrained in future simulations. Naturally, as the organic vapor condensation depends on the initial RH, is ΔCDNC is also sensitive to the selection of the initial RH (Fig. A.1). If the initial RH is set to 60%, CDNC enhancements as high as 100% could be expected, while if the initial RH is set to 99% the enhancements are expected to range between 0 and 20%. This variation is greater than what the ideality assumption (or the selection of vaporization enthalpy) poses on ΔCDNC (Sect. 3.1)."

5. In sections 3.3 and 3.4 the frequencies of the criteria for significant impact were analyzed one by one. What about the frequency of all the criteria fulfilled at the same time?

Reply: We apologize for not fully comprehending what the reviewer means about analyzing the criteria one by one. The criteria $D_2/D_1 < 6$ and $N_1 > 1000$ cm^{-3} are analyzed all together (Sect. 3.4), and that is shown in Fig. 5d for PARSEC-UFO simulations, and Fig. 7 for long-term SMEAR II measurements and UKESM1 (Sect. 3.5). We want to highlight that neither the dry PNSD surface area (S) threshold of 100 μm cm^{-3} (or $\sim s_{max} > 0.2\%$) or initial organic vapor concentration are used as criteria for identifying high ΔCDNC. The parameters are discussed together to show ***when the modeled ΔCDNC are sensitive to organic vapor concentration***.

6. Lines 708-710: "While the SMEAR II PNSD data are retrieved at ground level, utilization of the UKESM1 modal parameters (only soluble modes considered) from CB is chosen, because these PNSD log-normal parameters would actually meet the cloud droplet activation scheme in the model." - I find this selection a bit odd. Wouldn't it make more sense to look at the near-surface PNSD that would have a chance to grow with co-condensation in updrafts before cloud activation? How large is the difference between near-surface and BC PNSDs in UKESM?

Reply: Since co-condensation is not implemented in the model, and we are analyzing the dry PNSD, it would be the CB size distribution which would be relevant for a potential future co-condensation parameterization in the model i.e., co-condensation would affect only those aerosol populations which meet the activation scheme in UKESM1. ***Previous co-condensation parameterizations therefore also utilize the PNSD obtained at cloud base to account for co-condensation*** (Connolly et al., 2014; Crooks et al., 2018). ***PNSD near surface evolve in numerous ways within the UKESM1 and in the real atmosphere before reaching cloud base.*** Future work should rather be targeted in understanding how frequently the measured PNSD$_{NUM}$ meet cloud base as such, which would help us assess the likelihood of large CDNC enhancements taking place in reality.

Manuscript edits:

"Next, the frequency to which the PNSD criteria ($D_2/D_1 < 6$ and $N_1 > 1000$ cm^{-3}) are fulfilled in the long-term size distribution measurements is examined. For this purpose, the same 6-year PNSD data set collected at SMEAR II fitted with two log-normal size distributions (Hussein et al., 2005) is utilized. The percentage of times the criteria are met is shown in Fig. 7a. The highest frequencies (30–40% of the time) are observed in April, May and September, which correlates with a high new particle formation (NPF) frequency at the site (Nieminen et al., 2014; Dada et al., 2017). The monthly median size distributions fulfilling the criteria are shown in Fig. 7c. They all clearly exhibit the lack of a Hoppel minimum, similarly to $PNSD_{NUM}$, and suggest a potentially high impact of newly formed particles on cloud properties through co-condensation. However, future work should rather be targeted in understanding how frequently the measured $PNSD_{NUM}$ meet cloud base as such, which would help us assess the likelihood of large CDNC enhancements taking place in reality. This is particularly important, because NPF typically takes place in sunny, non-cloudy days, which provides time for the $PNSD_{NUM}$ to evolve before exposed to cloud base and subsequent droplet activation. The results again clearly emphasize the need of accurate representation of aerosol size distributions and lifecycle in models (such as other CPMs or global circulation models, GCMs) to account for the impacts of co-condensation and the strong seasonality to be expected in the magnitudes in ΔCDNC."

"In this section the SMEAR II results are compared against a 5-year UKESM1 simulation (see Sect. 2.4; analysis restricted to the boreal biome). While the SMEAR II PNSD data are retrieved at ground level, utilization of the UKESM1 modal parameters (only soluble modes considered) from CB is chosen, because these PNSD log-normal parameters would actually meet the cloud droplet activation scheme in the model. Previous co-condensation parameterization schemes have also been developed to treat the CB PNSD to account for co-condensation (Connolly et al., 2014; Crooks et al., 2018)."

Reviewer #2

General comment

This study investigates how cloud droplet number concentrations (CDNC) are altered through co-condensation of organic vapours along with water vapour during cloud events in boreal biomes. It uses an adiabatic cloud parcel model (ICPM), which is initialized at 90 % RH to simulate cloud formation in upraising air at updrafts of 0.1, 0.3, and 1 m/s. The simulation of the biogenic organic aerosol is based on volatility basis sets derived from measurement data of gas phase and condensed phase composition performed in the boreal forest of Finland during Spring 2014. A median enhancement in CDNC of 20 % was

predicted, and the most suitable conditions for a strong CDNC enhancement through co-condensation were found to occur in the presence of a nascent ultrafine aerosol mode, conditions occurring quite frequently in fall and spring. To come to this conclusion, the authors performed 97 ICPM simulations representing the atmospheric conditions: temperature profile, aerosol composition, and particle number size distribution (PNSD) fitted as an Aitken and an accumulation mode. Each simulation was initialized at the height and temperature where 90 % RH is reached and then run at the three pre-defined updrafts. The PNSD and aerosol chemical composition (gas and condensed phase) measured near ground level were taken to be identical to those at 90 % RH. Like this, PNSD, volatility distributions and temperature were different for every simulation. This variation in conditions makes the explanation of the model initialization and the interpretation of the results quite complex, and at times confusing. As the topic of this study is highly relevant and this study is the first one to simulate co-condensation in such detail, the method description especially the adaptation of the VBS to the starting temperature and the ICPM initialization need to be improved. Altogether, this is a very thorough study that deserves publication in ACP.

We thank the reviewer for this encouraging statement and the very thorough comments that helped us to significantly improve the manuscript!

We agree that the interpretation of the results has not been the easiest due to the chosen approach. However, this methodology enabled us to examine conditions that were actually taking place in the boreal forest environment (for example that under high initialization temperatures, the concentration of organic vapors is high, the aerosol mass is dominated by organic aerosol, and aerosol size distribution contains a large accumulation mode). Alternatively, we could have performed a more extensive analysis where the full parameter space was explored and highlighted the space (similarly as Lowe et al., 2019) with the most likely parameter combinations being highlighted. However, during the initial experiment design, ICPM was too slow to perform such high number of simulations (the 97 simulations with three updraft velocities took approximately seven days). Now, with the upgrade to PARSEC-UFO, the simulations are much faster (ca. 5 hours for the set of simulations) and one could perhaps study a wider parameter space while also further optimizing the number of volatility basis set bins included. This could be an interesting topic of future work.

ICPM initialization

1. **Information about the ICPM initialization is spread over the whole manuscript and can sometimes be inferred only indirectly. This hampers the reading and understanding of the manuscript.**

   Reply: Thank you for pointing this out. We have worked on improving the clarity.

   Manuscript edits:

   L180– L573 (structure changes):

   2 Methods and data
         2.1 The adiabatic cloud parcel model (PARSEC-UFO)
         2.2. PARSEC-UFO initialization and simulation setup
         2.3. PARSEC-UFO input data measurements and processing
               2.3.1. Volatility distributions from ACSM data (CJ distributions)

L256–L308 (fully adjusted):

"2.2 PARSEC-UFO initialization and simulation setup

The simulations shown within this work are performed with PARSEC-UFO with or without co-condensation. Initially, before the start of the adiabatic ascent, an initialization takes place in PARSEC-UFO. This involves the calculation of the binned wet particle number size distribution and in the case, where co-condensation is enabled, the initialization of the volatility distribution of organics. The binned wet PNSD is calculated using the parameters describing a dry log-normal PNSD (N_i, D_i, σ_i), information on aerosol chemical composition (mass fractions of chemical species), initial RH and temperature – all given as inputs for the model. When co-condensation is turned on, PARSEC-UFO takes in the summed volatility distributions (gas+particle phase i.e., $C_{g+p,q} = C_{g,q} + C_{p,q}$) –corrected for the PARSEC-UFO initialization temperature offline (Sect. 2.3) – as input. It then assumed upon the PARSEC-UFO initialization that the gas and particle phase are in equilibrium at the initialization RH. Finally upon initialization, PARSEC-UFO solves partitioning coefficients for each volatility bin (ξ_q) i.e., the distribution of organic mass between gas and particle phase:

$$\xi_q \equiv \frac{C_{p,q}}{C_{p,q} + C_{g,q}}, \tag{14}$$

where the total particle phase organic mass concentration across all volatility bins is

$$C_p = \sum_q C_{p,q} = \sum_q C_{g+p,q}\, \xi_q \tag{15}$$

and the partitioning coefficients depend on C^* as follows

$$\xi_q = \frac{C_p}{C_p + C_q^*}. \tag{16}$$

Each ξ_q is solved iteratively from Equations (15–16) following absorptive partitioning theory including water (Barley et al., 2009), as it was done by Topping et al. (2013) assuming equilibrium conditions. The iterative method is possible, as C_p is constrained by the initial PNSD and the organic mass fraction, and the relative proportions of the volatility bins (volatility distribution shape) are preserved. As assuming equilibrium conditions limits the amount of organic vapor available for co-condensation, it may also reduce the cloud response to co-condensation. Therefore, the initial organic vapor concentrations provided here can be taken as a lower limit.

Overall, 97 daytime scenarios (local time between 10:00 and 19:00) are simulated adiabatically with PARSEC-UFO. The initialization data originate from the Biogenic Aerosols – Effects on Clouds and Climate (BAECC) campaign, which took place in 2014 at the Station Measuring Ecosystem–Atmosphere Relationships (SMEAR) II in Hyytiälä, Finland (Petäjä et al.,

2016). The measurements and data processing relevant to this study are described in Sect. 2.3. The configuration of PARSEC-UFO used in this study only considers the adiabatic ascent of an air parcel, without treatment of variable vertical updraft during ascent, droplet collision and coalescence or entrainment. The simulations are performed for fixed updraft velocities of 0.1 m s^{-1}, 0.3 m s^{-1}, and 1.0 m s^{-1}, with and without co-condensation. During the CPM simulation period, SMEAR II was under daytime clouds roughly 50–60% of the time (Ylivinkka et al., 2020), which were most often low level clouds motivating selection of updraft velocities. The initial atmospheric pressure and relative humidity are set to 980 hPa and 90%, respectively, in all simulation scenarios, unless otherwise stated. The PARSEC-UFO initialization temperature varies throughout the simulation set, and is taken from interpolated radiosonde data that represents the 90% initialization (Sect. 2.3). The selection of the 90% RH was motivated by the previous study by Crooks et al. (2018). However, we acknowledge that more work is needed to better harmonize this parameter, along with initialization pressure, to in-situ aerosol measurements. Each modelled scenario has log-normal parameters describing a bimodal aerosol size distribution form BAECC measurements and the organic mass fraction from ACSM measurements (Sect. 2.3). The rest of the mass is assumed to be ammonium sulfate, which is generally a good approximation for SMEAR II (Heikkinen et al., 2020). For the simulations performed here, BC is not included given its small (about <5%) contribution to aerosol mass from late spring to summer (Luoma, 2021). While PARSEC-UFO does not utilize κ-Köhler theory (Petters and Kreidenweis, 2008), it might be useful to know that the assumed hygroscopicity, if translated to the hygroscopicity parameter κ, would be 0.14 and 0.72 for organics and ammonium sulfate, respectively (ideal solution; median $\kappa_{tot} \approx 0.32$). The assumed overall hygroscopicity is therefore likely to be overestimated, and it would exceed κ determined for SMEAR II experimentally in previous studies (e.g., Sihto et al., 2011 suggest $\kappa = 0.18$). Due to the likely overestimation of aerosol liquid water at initial conditions, it is also likely that the amount of organic vapor available for co-condensation after PARSEC-UFO initialization is underestimated.

Table 1 contains a summary of the simulation input data along with the values used for mass accommodation coefficient, surface tension, the vaporization enthalpy and effective soluble fraction of organics as well as the number of PNSD size bins. A more comprehensive look into the input data can be found in Table S.1. The simulation output at 50 m above cloud base, discussed later in the results section of the paper (Sect. 3), is summarized in Table 2. Particles exceeding the critical radius (calculated by Köhler theory) in their wet radii are considered as cloud droplets in this work. The output data are averaged to a fixed height output grid spaced with a two-meter resolution until 200 meters above cloud base. "

2. **On line 423, it is stated that an internal mixture of organics and ammonium sulfate (AS) is simulated, but the amount of AS in each simulation is not mentioned nor is the role of AS in co-condensation discussed.**

Reply: We thank the reviewer for this interesting point. Ammonium sulfate increases the aerosol water content at PARSEC-UFO initial conditions, which limits the amount of organic vapor available for co-condensation.

Manuscript edits:

L294–301:

"While PARSEC-UFO does not utilize κ-Köhler theory (Petters and Kreidenweis, 2008), it might be useful to know that the assumed hygroscopicity, if translated to the hygroscopicity parameter κ, would be 0.14 and 0.72 for organics and ammonium sulfate, respectively (ideal solution; median κ_{tot} ≈ 0.32). The assumed overall hygroscopicity is therefore likely to be overestimated, and it would exceed κ determined for SMEAR II experimentally in previous studies (e.g., Sihto et al., 2011 suggest κ = 0.18). Due to the likely overestimation of aerosol liquid water at initial conditions, it is also likely that the amount of organic vapor available for co-condensation after PARSEC-UFO initialization is underestimated."

3. **For the CJ distributions, it is stated on line 333 that "After the temperature adjustments, the volatility distributions are binned to ranges between $\log_{10}C^* = [-8, 3]$ spaced by one decade in C*". Comparing the VBS displayed in CJ with the ones labelled as CJ in Fig. 2a, similarities are difficult to detect. Figure 2 in CJ displays in 11 panels different VBS. All of them show constant low organic mass in the bins below $\log C^* = -1$ and increasing or even steeply increasing organic mass in the bins from $\log_{10}C^* = 0$ to 3. Topping et al. (2013) also displays a VBS with strongly increasing organic mass in $\log_{10}C^* > 0$ in their Fig. 2. This is opposite to the VBS distribution labelled as CJ in Fig. 2a. Why is this? To correctly adjust the VBS from CJ to the lower ICPM initialization temperature, information of the volatility bins with $\log C^*$ between 4 and 6 at 298°C would be required, but such data is not given in CJ. So, how could the temperature adjustment be performed at all?**

Reply: We respectfully redirect the reviewer from Fig. 2 (the 11 panels) to **Fig. 5e** in Cappa and Jimenez (2010). While the 11 panels in Fig. 2 have steeply increasing organic mass in the higher volatility bins, it should be kept in mind that these VBSs represent fresh SOA/POA (chamber generated aerosol etc.), while ***Fig. 5e represents LV-OOA***. LV-OOA dominates the daytime organic aerosol at SMEAR II (Heikkinen et al., 2021) and Fig. 2a in this manuscript highly resembles Fig. 5e in Cappa and Jimenez (2010), making it fully consistent with the literature. In general, it is so that the higher the OA volatility, the higher contribution of VBS bins from $\log_{10}C^* = [0, 3]$ in CJ style VBSs. As LV-OOA is a low-volatility OA type, mass is distributed in the low-volatility bins. OA from diesel exhaust, for example, is a more volatile OA type than LV-OOA, and this is why the VBS describing diesel exhaust OA has mass distributed to $\log_{10}C^* = [0, 3]$ (e.g., Cappa and Jimenez, 2010, Fig. 2k).

To bring some more clarity on the volatility bin adjustments, the reviewer is redirected to Eq. (13) and the plotting scripts for Fig. S.3 and Fig. S.7a are provided below.

As input, eq. (13) uses the *C** under 298K (reference temperature), which would be

```matlab
%% cstar under reference temperature (298K):
cstar_ref = 10.^(-6:1:3); % ug/m3
```

Each of the 10 volatility bins has an assigned signal contribution. See two examples:

```matlab
%% 1. First example

%ctot similar to Topping et al. (2013) main text (ctot_topping):
ctot_topping = [0.11 0.11 0.11 0.12 0.12 0.12 0.18 0.22 0.43 1.2];

%% 2. Second example

%ctot similar to BAECC (ctot_mix):
% ctot LV-OOA:
ctot_LV = [4 3 2.2 1.5 1 0.5 0.25 0.1 0.05 0];
% ctot SV-OOA:
ctot_SV = [0 1.2 1.5 1.9 2.2 2.8 3.5 4.5 5.9 7.9];
% Assume 80% LV-OOA and 20% SV-OOA:
ctot_mix = 0.8*ctot_LV + 0.2*ctot_LV;
```

To use Eq. (13), the reference temperature (298 K), the new temperature (~PARSEC-UFO initialization temperature), the universal gas constant (R), and enthalpy of vaporization need to be defined:

```matlab
%% adjust cstar to new temperature (cstar_new):
T_ref = 298; % K
T_new = 280; % K
R = 8.31451; % J/(mol*K)
hvap = 150e3; % J/mol;
```

Note that hvap is constant only in this example. When F and CJ distributions are generated in the paper, the relation between cstar_ref and hvap_ref is accounted for using Eq (17; `hvap_ref = (-11.*log10(cstar_ref) + 129).*1e-3 J/mol;`).

```matlab
%To calculate cstar_new, i.e. cstar under 280K, we use Eq. (13):
cstar_new = cstar_ref.*exp(hvap/R * (1/T_ref - 1/T_new)); % ug/m3

%%Plot the VBS

figure();

subplot(1,2,1)

% Plot ctot_topping under t_ref:
bar(log10(cstar_ref), ctot_topping, 'LineWidth',1.5, 'EdgeColor','k',
'facecolor','b','barwidth', .6, 'facealpha', .5,'LineStyle', '--')

hold on

% Plot ctot_topping under t_new:
bar(round(log10(cstar_new)), ctot_topping, 'LineWidth',1.5,
'EdgeColor','k', 'facecolor', 'r','barwidth', .3,'facealpha', 1)

legend('298 K', '280 K');
```

```matlab
xlabel('log_{10}{\itC}^*');
ylabel('OA signal ');
title('Topping VBS');

subplot(1,2,2)

% Plot ctot_mix under t_ref:
bar(log10(cstar_ref), ctot_mix, 'LineWidth',1.5, 'EdgeColor','k',
'facecolor','b','barwidth', .6, 'facealpha', .5,'LineStyle', '--')

hold on

% Plot ctot_mix under t_new:
bar(round(log10(cstar_new)), ctot_mix, 'LineWidth',1.5,
'EdgeColor','k', 'facecolor', 'r','barwidth', .3,'facealpha', 1)

xlabel('log_{10}{\itC}^*');
title('20% SV-OOA, 80% LV-OOA VBS');
```

Manuscript edits:

L388–L402:

"To calculate the CJ distributions for the BAECC OA types, the LV-OOA, SV-OOA and primary organic aerosol (POA; taken as a mix of HOA and BBOA) from the SMEAR II ACSM long-term data set are utilized (Heikkinen et al., 2021). During BAECC, the organic aerosol comprised 63% LV-OOA, 32% SV-OOA and only 5% HOA on average. Using the time-dependent mass fractions of each OA type, mass-weighted average CJ volatility distributions for each of the model initialization scenarios (97 of them) are calculated. The CJ distribution shapes are taken from Cappa and Jimenez (2010), and they are provided under 298.15 K.

As the CJ volatility distributions have been reported for 298.15 K (Cappa and Jimenez, 2010), and PARSEC-UFO simulations are generally initialized at lower temperatures (Fig. 1c), accounting for the impact the temperature reduction has on C^* is necessary. The relationship between temperature and C^* is accounted for using the Arrhenius-type Clausius-Clapeyron relation (Eq. 13), where T is the ambient temperature in Kelvin (the PARSEC-UFO initialization temperature), and T_{ref} is 298.15 K. For the relationship between ΔH_{vap} and C^* (T_{ref}), the formulation provided in Epstein et al. (2010) is used:

$$\Delta H_{vap} = -11 log_{10} C^* (T_{ref}) + 129, \qquad (17)$$

where ΔH_{vap} is the change in heat (enthalpy) of vaporization in kJ mol^{-1}. A lower limit of 20 kJ mol^{-1} is set to the ΔH_{vap}, which is close to the ΔH_{vap} determined for formic acid (NIST Chemistry WebBook, 2022). Eq. (17) would otherwise provide too low, unphysical and even negative values. The temperature adjustment (Eq. 13), does not change the shape of the volatility distribution, but the volatility distribution x-axis shifts to the left. See example in Fig. S.2. After the temperature adjustments, the volatility distributions are binned to ranges between $log_{10}C^*$ = [-8, 3] spaced by

one decade in C^*. The lower limit is reduced by two orders of magnitude ($C^*(T_{ref}) = [-6, 3]$), but the upper limit remains as the initialization temperatures did not exceed T_{ref}. The campaign average CJ volatility distribution is shown with black bars in Fig. 2a. However, each simulation utilizes a unique distribution constructed using the LV-OOA, SV-OOA, and POA time series."

Supplementary Figure 2:
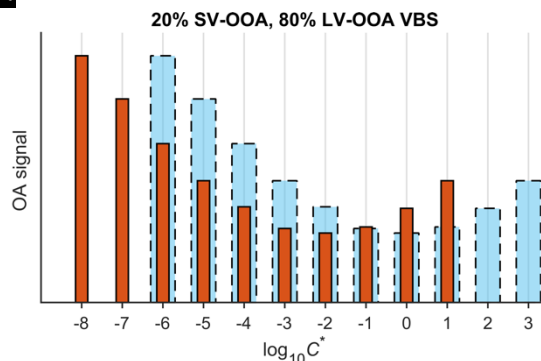
Figure S.3 *(a) A volatility basis set representing 20% SV-OOA and 80% LV-OOA. The blue dashed bars represent the volatility distribution under 298K and the red bars represent the BAECC PARSEC-UFO initialization temperature mean: 280K. The $log_{10}C^*$ axis is shifted according using Eq. (13) found in the main text of the paper. A constant enthalpy of vaporization is used for this example, but in the construction of CJ and F volatility distributions, enthalpy of vaporization depends on $log_{10}C^*$ (298K; Eq. 17).*

4. **Hunter et al. (2017) display in their Fig. 1c VBS derived from different measurement techniques including a gas-phase and a condensed-phase CIMS. The VBS derived from CIMS (g) data is very different from the one derived from PTR-MS for the same volatility range. As the choice of VBS is crucial for co-condensation, the derivation of this VBS needs to be explained better.**

Reply: We thank the reviewer for pointing this out. The Hunter et al. (2017) VBS is not used in PARSEC-UFO simulations. PTR-MS data are excluded from Hunter et al. (2017) data displayed in Fig. 2a. We have added a clarification in the manuscript (see below).

Manuscript edits:

L444–L452:

"The average F distribution shows a remarkable agreement with the organic volatility distributions from the BEACHON-RoMBAS field campaign conducted at the Manitou Experimental Forest Observatory in the Colorado Rocky Mountains in summer 2011 (Hunter et al., 2017, see Fig. 2a). Initially, Hunter et al. (2017) derived a volatility distribution for the total atmospheric reactive carbon (other than CH_4, CO_2 and CO) using six different types of measurements and assuming minimal overlap among the measured species. Here, the Hunter et al. (2017) distribution is displayed in Fig. 2a after shifting it to the mean PARSEC-UFO initialization temperature (280 K) using Eq. (13) and subtracting non-oxygenated VOC signals from it for comparison. The Hunter et al. (2017)

distribution is not used in PARSEC-UFO simulations, it is only shown for comparative purposes due to its similarity with the F distributions."

5. **For the F distribution, an adjustment to the initialization temperature is mentioned on line 370. How exactly was this adjustment carried out? How were the ΔH$_{vap}$ for the adjustment determined?**

Reply: Thank you for this comment and spotting our mistake. ΔH_{vap} depend only on the reference temperature (298K). Only Eq. (13) is used for T adjustments. Eq. (17) is removed when T adjustments mentioned throughout the manuscript, and it is clear that Eq. (13) is solely used for this purpose.

6. **Was a full equilibration carried out at the initialization temperature and RH? If yes, kinetic effects would only become important for the increase of RH from 90 % to 100 % and equilibration could be overestimated. The opposite would be the case if no equilibration were carried out at model equilibration. Can you comment on this?**

Reply: A full equilibration was performed similar to in Topping et al. (2013), and yes – the kinetic effects are only important from 90% to 100% RH. In reality, initial equilibrium conditions may not be reached and more organic vapor could remain in the gas phase at 90% RH. In such case, the modeled ΔCDNC could be greater in non-equilibrium conditions as opposed to equilibrium conditions due to the larger availability of organic vapor in the former. We can postulate that a larger initial organic vapor concentration would make a significant difference in the modelled ΔCDNC only under extremely clean conditions (Fig. 5c). We cannot provide an answer whether the environmental conditions sustaining a clean atmosphere would also promote non-equilibrium conditions. Motivated by this question, we added the following information to the manuscript.

Manuscript edits:

L270–L275:

"Each ξ_q is solved iteratively from Equations (15–16) following absorptive partitioning theory including water (Barley et al., 2009), as it was done by Topping et al. (2013) assuming equilibrium conditions. The iterative method is possible, as C_p is constrained by the initial PNSD and the organic mass fraction, and the relative proportions of the volatility bins (volatility distribution shape) are preserved. As assuming equilibrium conditions limits the amount of organic vapor available for co-condensation, it may also reduce the cloud response to co-condensation. Therefore, the initial organic vapor concentrations provided here can be taken as a lower limit. "

L288–L290:

"The selection of the 90% RH was motivated by the previous study by Crooks et al. (2018). However, we acknowledge that more work is needed to better harmonize this parameter, along with initialization pressure, to in-situ aerosol measurements."

L643–L658:

"As the results from Fig. 4 underline the time-dependence of co-condensation (Sect. 3.1), it is worth remembering that the PARSEC-UFO initialization RH is set to 90% where equilibrium conditions are assumed (see Sect. 2.4). Therefore, the kinetic effects play a role only from 90% to 100% RH. Importantly, if the initial RH was set to a lower value, more time would be available for co-condensation before reaching CB, and if the initial RH was set to a higher value, less time would be available. On the other hand, due to the assumption of initial equilibrium conditions, a lower initial RH also ensures a higher organic vapor concentration available for co-condensation, and a higher initial RH reduces the organic vapor availability. Together with initial temperature, the initial RH strongly control the amount of organic vapor available for co-condensation (Appendix A, Fig. A.1, Fig. S.3) and thereby the amount of soluble organic mass yielded by the time the air parcel reaches cloud base. While the decision of maintaining a fixed initial RH for the different simulations is proven useful for this study as it eases the data interpretation process, it should be acknowledged that the initial RH could be better constrained in future simulations. Naturally, as the organic vapor condensation depends on the initial RH, is ΔCDNC is also sensitive to the selection of the initial RH (Fig. A.1). If the initial RH is set to 60%, CDNC enhancements as high as 100% could be expected, while if the initial RH is set to 99% the enhancements are expected to range between 0 and 20%. This variation is greater than the impact the ideality assumption (or the selection of vaporization enthalpy) has on ΔCDNC (Sect. 3.1; Appendix A)."

7. **On line 162, it is stated that PNSD were constructed at model initialization. Then, on line 236, it is stated that "The PNSD for the ICPM initialization are obtained from the Differential Mobility Particle Sizer (DMPS) measurements from SMEAR II performed within the forest canopy." Do these measurements reflect the actual temperature at the forest canopy and dry conditions? Were they adjusted to reflect 90 % RH?**

Reply: Thank you for this comment. We hope this is now clarified in the improved description of the model initialization. The modal parameters (N_1, D_1, σ_1, N_2, D_2, σ_2) were obtained from fitting two modes to PNSD from DMPS measurements (dried, sampling height 8 meters above ground level, T = sampling height temperature). PARSEC-UFO takes in these modal parameters and then constructs a binned size distribution out of those (here 400 size bins between 2 nm and 5 µm). Prior to the start of the adiabatic ascent, PARSEC-UFO accounts for the initial relative humidity set to 90% and calculates the wet PNSD. The effect temperature may have on the wet PNSD is not accounted for as the organic mass fraction remains fixed when the partitioning coefficients are iterated prior to the adiabatic ascent.

8. **One general weakness in the discussion of the results is that the role of temperature and RH for the condensation of organic species is not kept properly apart. The effect of the lower temperature is e.g. shown in Fig. 4, panels g-i, but in the discussion of co-condensation depending on the season, the influence of temperature on ΔCDNC is not mentioned. If a full temperature adjustment had been carried out at model initialization, a temperature dependence as shown in Fig. 4 should not be present. The question therefore remains to what degree the higher co-condensation in spring and autumn compared with summer is caused by the lower temperatures during these seasons. In a revised manuscript version, the respective role of temperature and co-condensation should be discussed more explicitly.**

Reply: Thank you for this comment. See our response to the general comment regarding the simulation design. Some temperature dependency exists for organic vapor condensation due to Eq. (13), but the reviewer is right and the dependency shown in Fig. 4 panels g–i was not correct. Thinking about this comment helped us to discover a bug in ICPM-UFO, which was related to an inconsistency between the $\log_{10}C^*$ given as input for the model under the ICPM-UFO initialization temperature, but within the model it was treated as if it corresponded 298 K. After fixing the inconsistency, the temperature-dependence of IVOC condensation disappeared. Now IVOC condensation shows strong dependency on condensation sink ($\sim s_{max}^{-1}$). Therefore, **panels g–i are now removed from Fig. 4**, and the fraction of organic vapor (in the $\log_{10}C^*=7$ volatility bin) condensed before the air parcel has reached cloud base vs. the maximum supersaturation gained during the ascent is added to the supplementary material (Fig. S.4). Concerning the initial RH and T dependencies of the modelled ΔCDNC, we have added some sensitivity studies. **We show how the selection of initial T impacts the organic vapor concentration (Figs. S.8a** and **S.2** – discussed earlier within this document) **and show a how ΔCDNC changes under constant initial T, but varying initial RH (Appendix A, Fig. A.1** – discussed earlier within this document).

Manuscript edits:

Supplementary Figure 4:
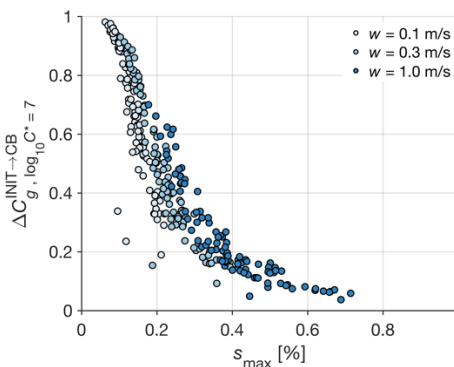
Figure S.4 *The fraction of organic vapor (in the $\log_{10}C^*=7$ volatility bin) condensed before the air parcel has reached cloud base vs the maximum supersaturation gained during the ascent. The darkest markers indicate simulations performed with an updraft velocity of 1.0 m s-1, the light blue markers correspond the updraft velocity of 0.3 m s.1 and the white markers the updraft velocity of 0.1 m s-1. If a high maximum supersaturation is reached, the condensation sink is low, and less*

IVOCs condense. If the maximum supersaturation is high, the condensation sink is high, and more IVOCs condense.

9. **On lines 493–501, the potential influence of non-ideality on gas-particle partitioning of organics is discussed. Despite recognising the shortcomings due to the assumption of ideality, quite detailed predictions of the co-condensation effect in boreal regions are made without taking the issue of solution non-ideality up again. A discussion of this aspect should be part of a revised discussion. The O:C could be estimated from CIMS and AMS data given in Fig. 2f. Such an estimate is strongly recommended to improve the manuscript.**

   Reply: We redirect the reviewer to the author response given to Reviewer #1 regarding the 7th bullet.

10. **Uncertainties in the PNSD should also be critically assessed as these were highlighted to be crucial to determine ΔCDNC. Bimodal fits (Aitken and accumulation modes) have been performed to describe the measured PNSD from the SMEAR II campaign although the monthly averages seem to be rather unimodal for some months. It would be instructive if the bimodal fits were shown at least for some typical examples (including a seemingly unimodal PNSD) in the SI.**

   Reply: We thank the reviewer for the comment. The normalized root mean squared error (NRMSE) between the measured PNSD and the PNSD constructed using the log-normal parameters for the bimodal fit is roughly 50% for the aerosol size range of interest. **The fitting algorithm by Hussein et al. (2005) first attempts fitting two modes (as two was set by us as the maximum number of modes), and then it mathematically evaluates whether the number of modes could be reduced to one**. **For all the scenarios, two modes were present yet the second mode is at times extremely minor.** We have added statistics of the fitting performance in the supplementary material (Fig. S.1) with four example fits including simulation #64 that could be perhaps interpreted as a monomodal PNSD by a brief glance. Regarding uncertainty, it seems that the fitting algorithm has priority on getting the total particle number concentration correct over the general shape of the PNSD. Therefore, it seems that the fitting procedure diminishes the gaps between different aerosol modes, such as the Hoppel minimum. PNSD with Hoppel minima were shown to yield lowest ΔCDNC. Therefore, this could have an impact on the modelled ΔCDNC. Hoppel minima is typically placed between 90–100 nm (dry diameter), which are close to the smallest activated dry diameters in our simulations. As the fitting procedure increases slightly the number of particles within this region, it may cause larger CDNC enhancements to take place. Perhaps including more than two modes could minimize this problem.

   Manuscript edits:

   L332–339:

   "For the BAECC data set, the optimal number would always be between three and four modes, with a higher number of modes generally yielding a better fit to the observational data as expected. Despite the optimal number of 3–4 modes, the maximum number of modes is restricted to two as the agreement between the fitted and measured distributions remained good considering the

experimental uncertainties (Fig. S.1). Statistics regarding the log-normal parameters of the fitted data during BAECC are provided in Tables 1 and S.1. The bimodal PNSD fits are also calculated for the years 2012–2017. These data are used later to evaluate the frequency of times size distributions yielding high ΔCDNC appear in long-term in-situ data."

Supplementary Figure 1:
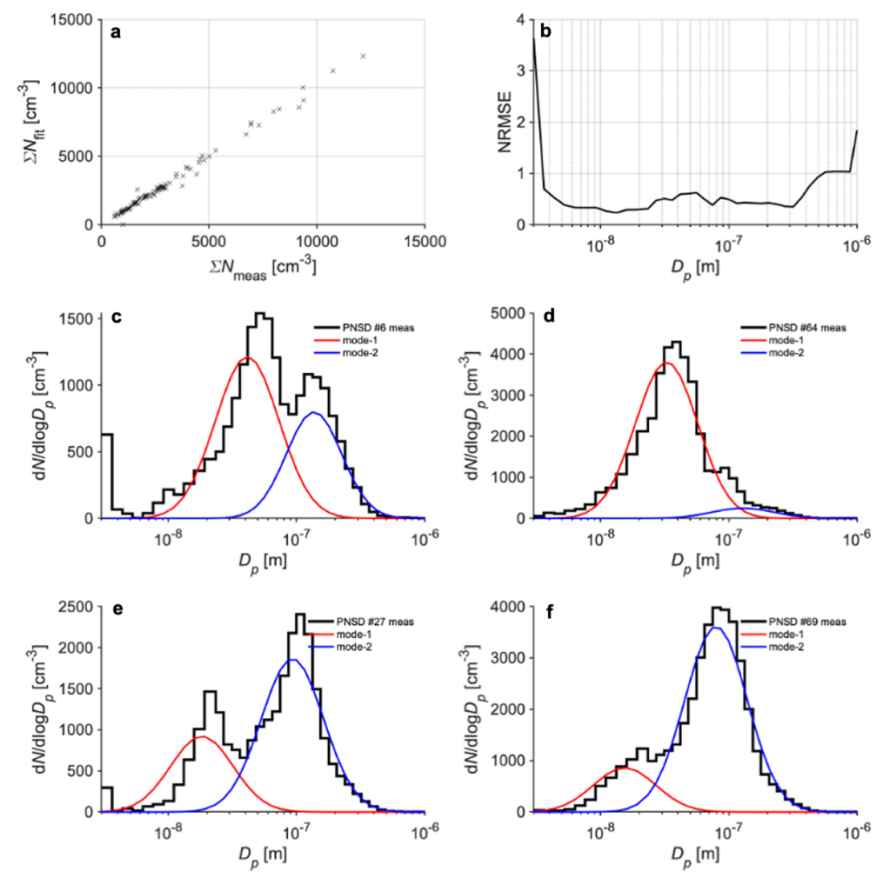
Figure S.1 *(a) A scatter plot between the number concentration of aerosol particles retrieved from the bimodal fits (y-axis) and the original DMPS measurements (x-axis). (b) The normalized root mean squared error (NRMSE) as function of particle dry diameter for the bimodal fits. (c–f) Bimodal fit examples are drawn over the observed black PNSD."*

11. **Aerosol properties are discussed in detail to estimate the effect of co-condensation over the boreal biome. While this discussion is very detailed, a discussion of the meteorological conditions in the boreal biome is missing: how often are there clouds at all? What updrafts prevail?**

Reply: It is correct that the meteorological conditions are discussed to a limited extent in this work, mostly because they are less well constrained as opposed to the aerosol properties. The updraft velocities are in line with observed updrafts at SMEAR II (personal communication with Prof. Dmitri Moisseev, Ranjan et al., in prep., 2024). The updraft velocity data preparation is laborious and therefore on-going, which is why the data are not included in this work and will not be discussed at such early stage. Cloudiness during

BAECC is discussed in Ylivinkka et al. (2020), and it reveals that during the PARSEC-UFO simulation period the daytime cloudiness was roughly 50–60%. However, note that cloudiness is typically low when $PNSD_{NUM}$ are measured and highest $\Delta CDNC$ modelled (comment to Reviewer #1, 9th bullet).

Manuscript edits:

L282-L290:

"The simulations are performed for fixed updraft velocities of 0.1 m s^{-1}, 0.3 m s^{-1}, and 1.0 m s^{-1}, with and without co-condensation. During the CPM simulation period, SMEAR II was under daytime clouds roughly 50–60% of the time (Ylivinkka et al., 2020), which were most often low level clouds motivating selection of updraft velocities. The initial atmospheric pressure and relative humidity are set to 980 hPa and 90%, respectively, in all simulation scenarios, unless otherwise stated. The PARSEC-UFO initialization temperature varies throughout the simulation set, and is taken from interpolated radiosonde data that represents the 90% initialization (Sect. 2.3). The selection of the 90% RH was motivated by the previous study by Crooks et al. (2018). However, we acknowledge that more work is needed to better harmonize this parameter, along with initialization pressure, to in-situ aerosol measurements. "

Specific comments

The nomenclature is not always consistent or clear throughout the manuscript:

12. **Sometimes s_c (lines 608–612; Fig. 3b) is used and sometimes s* (e.g. line 90). s* is defined as critical supersaturation but no definition is given for s_c. Is both critical supersaturation? If this is the case, the nomenclature should be made consistent.**

    Reply: Thank you for noticing. This has been corrected.

13. **What is the definition of r* (e.g. line 549)? Usually, it is defined as the critical radius, but for this, the values given in the text seem too low. Rather, it seems to be the smallest radius that becomes activated during cloud droplet activation. In Table 2, r^*_{noCC} and r^*_{CC} are defined, but a definition of r* is lacking.**

    Reply: Thank you for noticing. *r** is the smallest activated dry radius. This has been clarified.

14. **What is the definition of SVOC and IVOC in terms of volatility bins? Does the definition depend on the vapour pressure at the initialization temperature or at the vapour pressure at 300 K? The exact definition is e.g. important for the understanding of Fig. 3a.**

    Reply: Thank you for noticing. **SVOCs have $\log_{10}C^* = [0, 2]$ and IVOCs $\log_{10}C^* = [3, 7]$ under 279K**. Information added to Fig. 3 caption.

15. **Line 43: "suppression of the critical supersaturation": this sounds a bit too strong. It is rather just a "lowering".**

Reply: Thank you for the comment. We have changed the wording throughout the manuscript.

16. **Lines 88–89: As examples of direct experimental studies of co-condensation, Wang et al. (2020) and Gunthe et al. (2021) could be mentioned here. Wang et al. (2020) described a haze event in Beijing, which was driven by co-condensation of nitrate. Gunthe et al. (2021) describes a haze event in Delhi driven by co-condensation of HCl.**

Reply: Thank you for the suggestion.

Manuscript edits:

L113-L120:

" *Direct experimental studies of co-condensation remain challenging, however, as aerosol particles are typically dried during the sampling process and the loss of liquid water may lead to evaporation of co-condensed organics, too. While direct observational evidence of co-condensation is scarce, recent laboratory studies show significant water uptake due to co-condensation of propylene glycol and water onto ammonium sulfate particles (Hu et al., 2018). In addition, ambient observations from Delhi and Beijing suggest co-condensation of hydrochloric acid (HCl) or nitric acid (HNO$_3$) with water vapor, respectively, to be of essence in reproducing particle hygroscopicities corresponding to the visibility measurements during haze events (Gunthe et al., 2021; Wang et al., 2020).''*

17. **Lines 108–109: formulation is unclear: what is meant by "the asymptote of the curve"?**

Reply: Plateau of the curve. We have reformulated it accordingly.

18. **Lines 182–185: In Eq. 5, the liquid water mixing ratio is calculated from the increase in particle radii due to condensed water mass. From the increase in radius, the additional volume can be calculated and converted to water mixing ratio. It is not clear why the particle dry mass should appear in the denominator. Rather, it should be the air density to convert to mixing ratio.**

Reply: Thank you, we have checked and corrected Eq. 5. See response to Reviewer #1, 3rd bullet.

19. **Lines 283–284: "The PNSD and aerosol chemical composition measured near ground level are assumed to be identical to those at 90 % humidity": Co-condensation between dry conditions and 90 % RH will change the size distribution. Is this neglected? See also general comment.**

Reply: See the improved description of PARSEC-UFO initialization (Sect. 2.2.; Reviewer #2, 1st bullet).

20. **Lines 194–203: in the calculation of the Köhler equation, ideality is assumed. This is mentioned but not fully discussed. See general comment.**

Reply: See the improved description of PARSEC-UFO initialization (Sect. 2.2.; Reviewer #2, 1st bullet) and Appendix A and associated discussion (Reviewer #1 7th bullet).

21. **Line 316: "of the three": are the three fitting parameters meant here?**

Reply: We have removed this sentence to improve manuscript flow, but "the three" were ΔHvap, mass accommodation coefficients and volatility distribution shapes.

22. **Line 345: the sentence structure should be checked.**
Reply: Checked and reformulated. Thank you.

23. **Lines 346, 352–360, and 401–415: here, the oxygenation of the organic compounds is discussed. The ACSM together with the CIMS information could be used to infer hydrophilicity and estimate the role of non-ideality in gas-particle partitioning. Eq. 18 requires information of oxidation state, thus the basis for such an estimate would be given. See also general comment.**

Reply: See Appendix A and associated discussion (Reviewer #1 7th bullet).

24. **Lines 369–376: How is the temperature adjustment of the volatility bins to the initial temperature done? Are the substances kept in the same bin and just assigned a lower vapour pressure or are the substances reassigned to the new bin with the correct C* at the temperature? This should be explained better. Could you comment here the role of fragmentation or dimerization of organic substances during the measurements?**

Reply: Yes, we believe the reviewer explains the procedure correctly. See response to Reviewer #2, 3rd bullet.

25. **Line 418 and Fig. 1a: the red crosses seem orange on my screen.**
Reply: Corrected. Thank you.

26. **Lines 418–423 and Table 1: what is the total mass of organics (gas and condensed phase; sum of all volatility bins) and ammoniums sulfate? This information should be given e.g. as additional rows in Table 1. Table 1 should be referenced in the text here.**
Reply: See Table 1 in SI. Can be calculated based on the information.

27. **Line 479: "gas-phase concentration" should be specified.**
Reply: Unfortunately, we cannot find "gas-phase concentration" mentioned on Line 479.

28. **Line 481: CB should be defined more exactly in terms of RH. In Fig. S2a, "below CB" seems to be taken as RH = 99.98 % RH. Was this the assumption throughout the manuscript? If yes, it should be stated in the main text.**
   Reply: CB is defined as RH = 100% (L529), but the model output rebinned to a 2-m resolution (L305–308). Therefore, the "below CB" contain all the saved outputs in subsaturated conditions. This has been clarified in Sect. 2.2 – see earlier replies.

29. **Lines 490–501: Here, the assessment of non-ideality by Topping et al. (2013) is discussed, and it is mentioned that the simulated co-condensation should be assessed with caution. Specifically it is stated "it is likely that solubility decreases towards the higher volatility bins." Nevertheless, in the elaboration of the relevant criteria for co-condensation, this caution was not kept up. The discussion of the role of non-ideality should be taken up again here. See also general comment.**
   Reply: See Appendix A and associated discussion (Reviewer #1 7th bullet).

30. **Line 504–509: up to 100 % of organic mass in volatility bin logC* = 7 has been found to condense below CB. This is a lot! At what temperature was the bin initialized (is it bin logC* = 7 at 300 K or at the initialization temperature)? If it is logC* = 7 at the initialization temperature, the condensation seems too large compared with Topping et al. (2013) when below CB is defined as 99.98 % RH. In Topping et al., less than 90 % of the bin logC* = 3 was condensed at 99.9999 % RH.**

   Reply: This is reduced now that the bug was corrected (see general comments in the beginning of the document). See panel b below, where the updraft velocity matches the Topping et al. (2013) simulation. Note that the direct comparison between Topping et al. (2013) results and ours is not straightforward. See also General information, 2nd bullet.
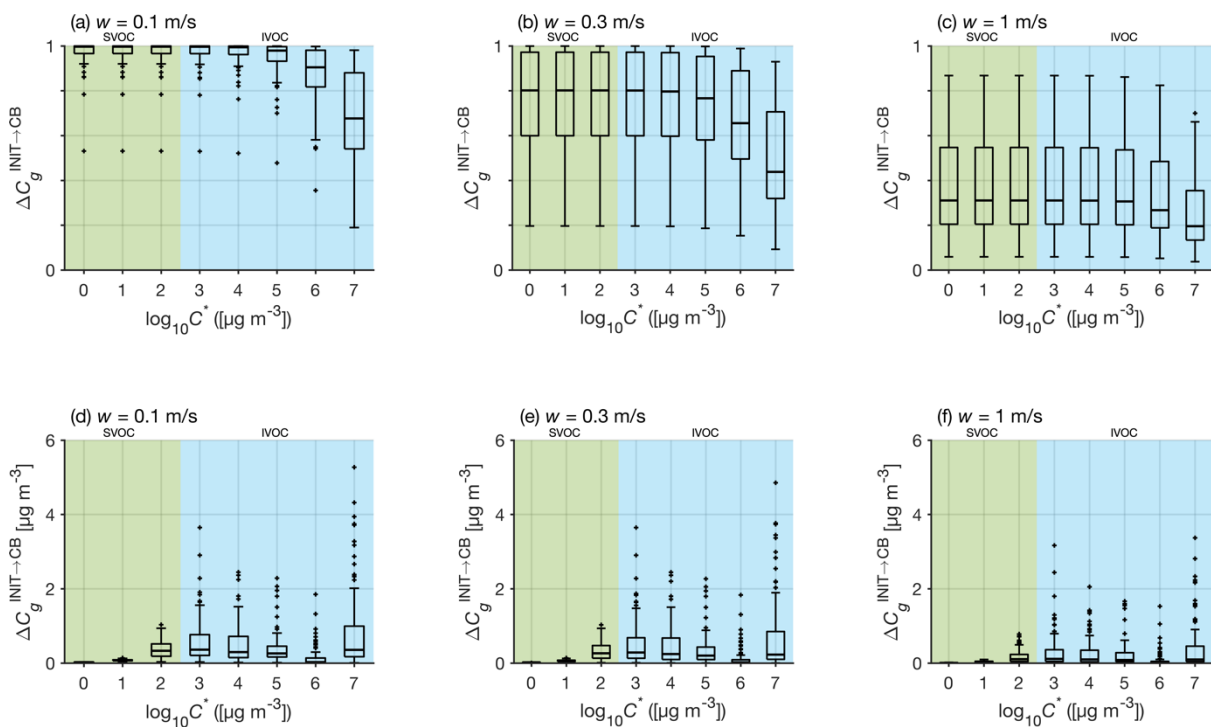
Figure 4 *Box plots showing the fractions (**a–c**) and absolute concentrations (**d–f**) of organic vapor condensed below cloud base per volatility bin for the 0.1, 0.3 and 1.0 m s⁻¹ updraft scenarios, respectively. The shaded backgrounds reflect SVOC (green) and IVOC/VOC (blue) volatility ranges under 298 K.*

31. **Lines 514–516: "The condensation efficiency of the highest volatility bin shows a high ICPM initialization temperature dependence. If the model initialization takes place at 270 K, up to 100 % of the organic vapor in the bin condenses, while if the ascent starts at 290 K, only 40 % of the mass concentration is transferred to the condensed phase below CB (Figs. 4g-i)": These two sentences seem to imply that the substances are assigned to bins at 300 K and this assignment is kept at lower temperatures. This would be opposite to the description of initialization in the method section.**

Reply: See response to Reviewer #2, 8th bullet.

32. **Line 549: r* has not been defined.**

Reply: See response to Reviewer #2, 13th bullet.

33. **Line 558: are "critical radii" r*?**

Reply: See response to Reviewer #2, 13th bullet.

34. **Line 561: susceptibility to what?**

Reply: We thank the reviewer. This has been clarified.

Manuscript edits:
L604-L605:

"The swarm plot on Fig. 5a shows that ΔCDNC and CDNC do not correlate i.e., low CDNC in the noCC runs does not favor high ΔCDNC. ."

35. **Line 571: what does not happen? The steep slope? Formulation should be improved.**

Reply: We thank the reviewer. This has been clarified by specifying that we investigate the PNSD dN/dD.

Manuscript edits:
L606-L620:

"On average during the BAECC simulation period (97 simulations), the highest ΔCDNC are found when initializing the model with a 0.3 m s^{-1} updraft velocity (also visible in Fig. 3d for the May 11 case) followed by ΔCDNC predictions for the 1 m s^{-1} case. In the latter, high supersaturations are achieved leading to the formation of many cloud droplets, yet the effects of co-condensation remained less pronounced as the high ascent speed poses kinetic limitations for organic condensation (see Sect. 3.1 and Fig. 4). Despite the highest organic uptake in the 0.1 m s^{-1} updraft simulations (Fig. 4a, d), the ΔCDNC remains the lowest. This can be explained by the low s_{max}, which remains insufficient to activate small particles to cloud droplets (r^*_{noCC} ~64 nm; Table 2). As the Aitken mode possesses most particles in terms of number (Table 1), the few nm reductions in r^* affect ΔCDNC the most when the r^* reduction takes place on the steep PNSD slopes (high dN/dD) between the Aitken and accumulation mode. When the updraft velocity is low (0.1 m s^{-1}), the r^* are too large to overlap with the parts of the PNSD with a high dN/dD even if r^* reduces greatly due to co-

condensation. Due to the high updraft-dependency of the modelled ΔCDNC, future process modeling work should consider performing simulations following updraft probability density functions (PDF), as used in GCMs, and calculating PDF weighted CDNC (West et al., 2014). This way more weight will be given to lower updrafts, and the model outputs will be more robust since the air parcels do not experience single updrafts in reality."

36. **Lines 579–581: "This result highlights that significant quantities of co-condensable organic vapors are distributed in the higher volatility bins and these concentrations should not be neglected in further co-condensation studies." This statement is questionable in view of Topping et al. who found ΔCDNC up to 55 % using volatility bins just up to logC* = 3 (as stated on line 577 of this manuscript). The role of the higher volatility bins should be elaborated further in view of the initialization temperature.**

    Reply: See general information, 2nd bullet and response to Reviewer #2, 8th bullet.

37. **Line 589: the median mode diameters of Aitken and accumulation modes should be mentioned here.**
    Reply: We thank the reviewer. This has been added (~40 nm for Aitken and ~110 nm for accumulation mode).

38. **Lines 595–597: "This result underlines that environments rich in particles from a local source would be more susceptible to high ΔCDNC due to co-condensation while regions with aged and cloud processed size distributions are affected less (ΔCDNC < 20% in our simulations; Fig. 5a)." This is a very general statement and might be questioned, considering that organic emissions from local sources are generally also less oxidized, which again would reduce co-condensation if non-ideality is considered.**

    Reply: We agree that it might be questioned, but we still stand by it. Based on this study, we could argue that the shape of the PNSD is one of the key factors influencing ΔCDNC (besides initial RH and *T*) and we could argue further that if there is a process sustaining the source of the particles and this PNSD shape, then there is also enough vapor present. In regions with new particle formation as the particle source, this would mean that the (organic) vapors also have undergone oxidation to be able to sustain in the particle growth. If we take environments dominated by anthropogenic emissions, it is likely that there is NO_x or ammonia present which can contribute to co-condensation (note that the sentence does not specify that the co-condensing species has to be organic) and if biomass burning as the source, the emissions contain many rather water-soluble species.

39. **Line 616: what is meant by "suppress the solute effect"? Bulk depletion by surface partitioning? "Suppression" is not mentioned in the cited study. It should be explained better what is meant and not just referred to Sorjamaa et al.**
    Reply: The reviewer is right, and our use of the word "suppression" is not appropriate throughout the manuscript. After a careful look at the PhD thesis of Samuel Lowe (Lowe, 2020), the speculation of the combined effects of surface active organics and co-condensation has been removed due to the complexity of the interplay.

Manuscript edits:

L689-L694:

"The sensitivity of the CDNC enhancements to PNSD$_{NUM}$ in this study as well as in Lowe et al. (2019) demonstrates that the activation of fresh and non-cloud-processed aerosol particles is susceptible to small reductions in s* that can be triggered e.g., by organic surfactants or co-condensation. Importantly, potential surface activity also affects the CCN activation behavior of atmospheric organics (Ruehl et al., 2012, 2016; Lowe et al., 2019), correlating with volatility and solubility. The combined effect of all these three properties needs to be thoroughly investigated in the future."

40. **Line 624: what is meant by "our results" here? Surface tension is not treated in the present study.**
    Reply: Thank you. We have added "[…] together with the Lowe et al. (2019) results […]".

41. **Line 645–647: this sentence is unclear. The connection between supersaturation, gas phase concentration of organics, and particle number should be explained better.**
    Reply: Thank you, we have improved the explanation as follows.
    Manuscript edits:

L712–L721:

"In addition to the PNSD$_{NUM}$ features, also the initial organic vapor concentration (C_g^{INIT}) influences the modeled ΔCDNC. The extent to which the modeled ΔCDNC are sensitive to C_g^{INIT} is depicted in Fig. 5c using the PARSEC-UFO simulations performed with 0.3 m s^{-1} updrafts. The y–axis represents the modeled ΔCDNC and the x-axis the organic vapor concentration distributed in log$_{10}$C* bins within [-4, 4] (denoted as $C_{g, -4:4}^{INIT}$) i.e., in bins that do not show high dependency on the available surface area (see Sect. 3.2 and Fig. S.4 for details). The relationship is not straightforward, but linear increases in ΔCDNC as a function of $C_{g, -4:4}^{INIT}$ can be seen under constant, yet sufficiently high s$_{max}$ (here >0.2%). Under the modelled scenarios, where s$_{max}$>0.2% the $C_{g, -4:4}^{INIT}$ is generally low (< 2 μg m^{-3}). Still, the highest CDNC enhancements during the BAECC simulation period are achieved under these conditions. The high CDNC enhancements can be achieved – despite the low organic vapor abundance simply because the soluble organic mass is distributed to more particles."

43. **Lines 654–657: Figure 3d shows a considerable effect due to co-condensation for updrafts of 1 m/s. Nevertheless, this updraft is not discussed at all in the next section. It should be mentioned how frequent supersaturations above 0.5 m/s are (or more generally the distributions of updrafts leading to cloud cover in Hyytiälä). If they are frequent, a discussion of higher updrafts should be added (including figures, e.g. as part of the SI).**

    Reply: The updrafts are generally below 1 m s^{-1} at SMEAR II during this time of the year. The clouds above the station are typically low-level clouds (Ylivinkka et al., 2020), where updraft velocities are also lower. Analysis of the updrafts will be subject of future work. See also response to Reviewer #3, 13th bullet.

44. **Line 697: do you mean "correlates with a high new particle formation frequency"?**
    Reply: Yes, thank you, this has been corrected.

45. **Lines 698–699, Fig. 7c and Sect. 3.5: all measured monthly PNSDs are very similar. None has a clear Hoppel minimum. In contrast, all simulated size distributions show a clear Hoppel minimum. The manuscript states that the co-condensation effect on droplet activation is very sensitive to the size distribution. How useful are then the UKESM1 simulations when they model the size distributions so differently from the measurements?**

    Reply: Thank you. See response to Reviewer #1, 6th bullet.

46. **Line 774: consider the word choice: "lowering" might be more adequate than "suppression".**

    Reply: Thank you. Corrected throughout.

47. **Figure 1c: what time of day has the temperature been measured?**

    Reply: At 06, 12, 18, 24 UTC. The interpolated radiosonde data product is used.

    Manuscript edits:

    L347–L349:

    "As PARSEC-UFO simulations are initialized at 90% RH, which is most of the time higher than that measured at ground level, an interpolated radiosonde data product from the BAECC campaign (ARM Data Center, 2014) is used to find temperatures matching 90% RH."

49. **Fig. 2b and c: is this the partitioning at dry conditions or at model initialization? This information should be added to the figure caption.**

    Reply: Yes, we have added this information. Thank you.

50. **Fig. 2d is not explained in the text. Does the displayed partitioning refer to a specific bin?**

    Reply: Thank you for the comment. The data points refer to 12 different volatility bins (12 data points shown). This is now stated in the Figure caption.

51. **Line 907: "in shown in": should this be: "is shown by"?**

    Reply: Corrected. Thank you.

52. **Line 918: "supersaturation -0.1%, RH=90%": how does this fit together?**

    Reply: Corrected. Thank you.

53. **Fig. 4d: the caption to this panel is missing.**

    Reply: Added. Thank you.

54. **Line 939: the figure caption and the legend within the figure do not give the same percentiles.**

    Reply: Corrected. Thank you.

55. **Figure 6a: the font of the legend is too small.**

    Reply: We have increased font size. Thank you.

Supplementary information:

56. **Figure S.2 The updraft should be explicitly stated. I guess it is 0.3 m/s?**

Reply: It is now stated 0.1 m s⁻¹ in the figure caption.

57. **Line 26: red lines seem orange on my screen.**
    Reply: We have updated the text to say orange/red. Thank you.

58. **Line 35: there is no red shaded size range.**
    Reply: Yes, there is. We have added details to the text and made it clear that the size of the shaded range is very small.

59. **Figure S.3: there is a lot of information in one plot. Consider to make additional plots with D2 against CDNC and D1 against CDNC. Like this, one could see better whether there is a correlation between these parameters.**
    Reply: Thank you for the suggestion. We have added the subplots.

Manuscript edits:
Supplementary figure 6:
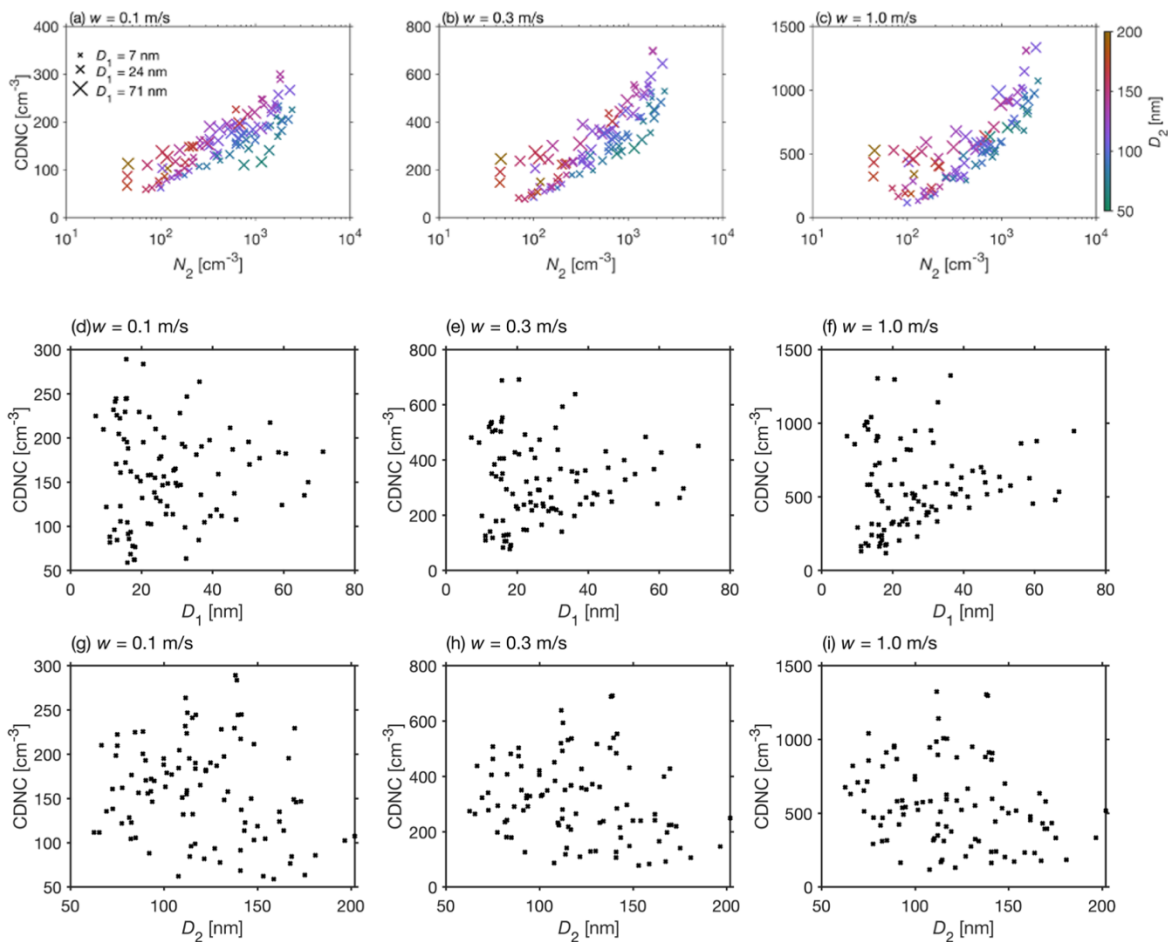
"*Figure S.6* The relationship between cloud droplet number concentration (CDNC; y-axis) and accumulation mode number concentration (N_2; x-axis), accumulation mode geometric mean diameter (D_2; color-coding), and Aitken mode geometric mean diameter (D_1; marker size) for the 0.1, 0.3 and 1.0 m s⁻¹ updraft scenarios, respectively (panels **a–c**) during BAECC. CDNC is obtained from simulations without co-condensation (noCC). N_2, D_2, and D_1 are used as model input data and represent the bimodal fits performed on the measured PNSD using the fitting algorithm by Hussein et al. (2005). Panels d–f and g–i show CDNC vs D_1 and D_2, respectively, for the different updraft velocities respectively."

61. **Line 53: "The markers from every 97 simulations are color-coded with the initial concentration of organic vapor in both simulation sets.": The legend within the panels states that it is the ratio between the two values. Please clarify which information is correct.**

   Reply: This figure has been removed (see general information before the review replies).

62. **Line 67: "(86% of the time in panel a, 78% of the time in panel b and 90% of the time for panel c)." The numbers within this bracket are confusing, as they suggest that most of the time the surface area exceeds 100 mm^{2}cm^{-3}. Instead, the given percentages give the frequencies for which the calculated surface areas are lower.**

   Reply: Thank you for spotting this, it has now been corrected.

63. **Figure S.6: In this figure, frequencies from 10 to 40 % seem abundant. Is this true or just due to the choice of color scale? If it were true, it is not discussed like this in the text.**

   Reply: This is true, but outside the boreal biome. For this reason, we have not discussed it in the manuscript.

References

Gunthe, S. S., Liu, P., Panda, U., Raj, S. S., Sharma, A., Darbyshire, E., Reyes-Villegas, E., Allan, J., Chen, Y., Wang, X., Song, S., Pohlker, M. L., Shi, L., Wang, Y., Kommula, S. M., Liu, T., Ravikrishna, R., McFiggans, G., Mickley, L. J., Martin, S. T., Poschl, U., Andreae, M. O., and Coe, H.: Enhanced aerosol particle growth sustained by high continental chlorine emission in India, Nature Geoscience, https://doi.org/10.1038/s41561-020-00677-x, 2021.

Wang, Y., Chen, Y., Wu, Z., Shang, D., Bian, Y., Du, Z., Schmitt, S. H., Su, R., Gkatzelis, G. I., Schlag, P., Hohaus, T., Voliotis, A., Lu, K., Zeng, L., Zhao, C., Alfarra, M. R., McFiggans, G., Wiedensohler, A., Kiendler-Scharr, A., Zhang, Y., and Hu, M.: Mutual promotion between aerosol particle liquid water and particulate nitrate enhancement leads to severe nitrate-dominated particulate matter pollution and low visibility, Atmos. Chem. Phys., 20, 2161-2175, https://doi.org/10.5194/acp-20-2161-2020, 2020.

Aalto, P., Hämeri, K., Becker, E., Weber, R., Salm, J., Mäkelä, J. M., Hoell, C., O'dowd, C. D., Hansson, H.-C., Väkevä, M., Koponen, I. K., Buzorius, G., and Kulmala, M.: Physical characterization of aerosol particles during nucleation events, Tellus B: Chemical and Physical Meteorology, 53, 344–358, https://doi.org/10.3402/tellusb.v53i4.17127, 2001.

Barley, M., Topping, D. O., Jenkin, M. E., and McFiggans, G.: Sensitivities of the absorptive partitioning model of secondary organic aerosol formation to the inclusion of water, Atmos. Chem. Phys., 9, 2919–2932, https://doi.org/10.5194/acp-9-2919-2009, 2009.

Cerully, K. M., Raatikainen, T., Lance, S., Tkacik, D., Tiitta, P., Petäjä, T., Ehn, M., Kulmala, M., Worsnop, D. R., Laaksonen, A., Smith, J. N., and Nenes, A.: Aerosol hygroscopicity and CCN activation kinetics in a boreal forest environment during the 2007 EUCAARI campaign, Atmospheric Chemistry and Physics, 11, 12369–12386, https://doi.org/10.5194/acp-11-12369-2011, 2011.

Connolly, P. J., Topping, D. O., Malavelle, F., and McFiggans, G.: A parameterisation for the activation of cloud drops including the effects of semi-volatile organics, Atmos. Chem. Phys., 14, 2289–2302, https://doi.org/10.5194/acp-14-2289-2014, 2014.

Crooks, M., Connolly, P., and McFiggans, G.: A parameterisation for the co-condensation of semi-volatile organics into multiple aerosol particle modes, Geosci. Model Dev., 11, 3261–3278, https://doi.org/10.5194/gmd-11-3261-2018, 2018.

Dada, L., Paasonen, P., Nieminen, T., Buenrostro Mazon, S., Kontkanen, J., Peräkylä, O., Lehtipalo, K., Hussein, T., Petäjä, T., Kerminen, V.-M., Bäck, J., and Kulmala, M.: Long-term analysis of clear-sky new particle formation events and nonevents in Hyytiälä, Atmos. Chem. Phys., 17, 6227–6241, https://doi.org/10.5194/acp-17-6227-2017, 2017.

Donahue, N. M., Robinson, A. L., Stanier, C. O., and Pandis, S. N.: Coupled Partitioning, Dilution, and Chemical Aging of Semivolatile Organics, Environ. Sci. Technol., 40, 2635–2643, https://doi.org/10.1021/es052297c, 2006.

Donahue, N. M., Epstein, S. A., Pandis, S. N., and Robinson, A. L.: A two-dimensional volatility basis set: 1. organic-aerosol mixing thermodynamics, Atmos. Chem. Phys., 11, 3303–3318, https://doi.org/10.5194/acp-11-3303-2011, 2011.

Guenther, A. B., Jiang, X., Heald, C. L., Sakulyanontvittaya, T., Duhl, T., Emmons, L. K., and Wang, X.: The Model of Emissions of Gases and Aerosols from Nature version 2.1 (MEGAN2.1): an extended and updated framework for modeling biogenic emissions, Geoscientific Model Development, 5, 1471–1492, https://doi.org/10.5194/gmd-5-1471-2012, 2012.

Gunthe, S. S., Liu, P., Panda, U., Raj, S. S., Sharma, A., Darbyshire, E., Reyes-Villegas, E., Allan, J., Chen, Y., Wang, X., Song, S., Pöhlker, M. L., Shi, L., Wang, Y., Kommula, S. M., Liu, T., Ravikrishna, R., McFiggans, G., Mickley, L. J., Martin, S. T., Pöschl, U., Andreae, M. O., and Coe, H.: Enhanced aerosol particle growth sustained by high continental chlorine emission in India, Nat. Geosci., 14, 77–84, https://doi.org/10.1038/s41561-020-00677-x, 2021.

Hallquist, M., Wenger, J. C., Baltensperger, U., Rudich, Y., Simpson, D., Claeys, M., Dommen, J., Donahue, N. M., George, C., Goldstein, A. H., Hamilton, J. F., Herrmann, H., Hoffmann, T., Iinuma, Y., Jang, M., Jenkin, M. E., Jimenez, J. L., Kiendler-Scharr, A., Maenhaut, W., McFiggans, G., Mentel, T. F., Monod, A., Prévôt, A. S. H., Seinfeld, J. H., Surratt, J. D., Szmigielski, R., and Wildt, J.: The formation, properties and impact of secondary organic aerosol: current and emerging issues, Atmospheric Chemistry and Physics, 9, 5155–5236, https://doi.org/10.5194/acp-9-5155-2009, 2009.

Heikkinen, L., Äijälä, M., Daellenbach, K. R., Chen, G., Garmash, O., Aliaga, D., Graeffe, F., Räty, M., Luoma, K., Aalto, P., Kulmala, M., Petäjä, T., Worsnop, D., and Ehn, M.: Eight years of sub-micrometre organic aerosol composition data from the boreal forest characterized using a machine-learning approach, Atmos. Chem. Phys., 21, 10081–10109, https://doi.org/10.5194/acp-21-10081-2021, 2021.

Hong, J., Häkkinen, S. a. K., Paramonov, M., Äijälä, M., Hakala, J., Nieminen, T., Mikkilä, J., Prisle, N. L., Kulmala, M., Riipinen, I., Bilde, M., Kerminen, V.-M., and Petäjä, T.: Hygroscopicity, CCN and volatility properties of submicron atmospheric aerosol in a boreal forest environment during the summer of 2010, Atmospheric Chemistry and Physics, 14, 4733–4748, https://doi.org/10.5194/acp-14-4733-2014, 2014.

Hu, D., Topping, D., and McFiggans, G.: Measured particle water uptake enhanced by co-condensing vapours, Atmospheric Chemistry and Physics, 18, 14925–14937, https://doi.org/10.5194/acp-18-14925-2018, 2018.

Huang, W., Li, H., Sarnela, N., Heikkinen, L., Tham, Y. J., Mikkilä, J., Thomas, S. J., Donahue, N. M., Kulmala, M., and Bianchi, F.: Measurement report: Molecular composition and volatility of gaseous organic compounds in a boreal forest – from volatile organic compounds to highly oxygenated organic molecules, Atmos. Chem. Phys., 21, 8961–8977, https://doi.org/10.5194/acp-21-8961-2021, 2021.

Hunter, J. F., Day, D. A., Palm, B. B., Yatavelli, R. L. N., Chan, A. W. H., Kaser, L., Cappellin, L., Hayes, P. L., Cross, E. S., Carrasquillo, A. J., Campuzano-Jost, P., Stark, H., Zhao, Y., Hohaus, T., Smith, J. N., Hansel, A., Karl, T., Goldstein, A. H., Guenther, A., Worsnop, D. R., Thornton, J. A., Heald, C. L., Jimenez, J. L., and Kroll, J. H.: Comprehensive characterization of atmospheric organic carbon at a forested site, Nature Geosci, 10, 748–753, https://doi.org/10.1038/ngeo3018, 2017.

Hussein, T., Maso, M. D., Petäjä, T., Koponen, I. K., Paatero, P., Aalto, P. P., Hämeri, K., and Kulmala, M.: Evaluation of an automatic algorithm for fitting the particle number size distributions, Boreal Environ. Res., 10, 19, 2005.

Jimenez, J. L., Canagaratna, M. R., Donahue, N. M., Prevot, A. S. H., Zhang, Q., Kroll, J. H., DeCarlo, P. F., Allan, J. D., Coe, H., Ng, N. L., Aiken, A. C., Docherty, K. S., Ulbrich, I. M., Grieshop, A. P., Robinson, A. L., Duplissy, J., Smith, J. D., Wilson, K. R., Lanz, V. A., Hueglin, C., Sun, Y. L., Tian, J., Laaksonen, A., Raatikainen, T., Rautiainen, J., Vaattovaara, P., Ehn, M., Kulmala, M., Tomlinson, J. M., Collins, D. R., Cubison, M. J., E., Dunlea, J., Huffman, J. A., Onasch, T. B., Alfarra, M. R., Williams, P. I., Bower, K., Kondo, Y., Schneider, J., Drewnick, F., Borrmann, S., Weimer, S., Demerjian, K., Salcedo, D., Cottrell, L., Griffin, R., Takami, A., Miyoshi, T., Hatakeyama, S., Shimono, A., Sun, J. Y., Zhang, Y. M., Dzepina, K., Kimmel, J. R., Sueper, D., Jayne, J. T., Herndon, S. C., Trimborn, A. M., Williams, L. R., Wood, E. C., Middlebrook, A. M., Kolb, C. E., Baltensperger, U., and Worsnop, D. R.: Evolution of Organic Aerosols in the Atmosphere, Science, 326, 1525–1529, https://doi.org/10.1126/science.1180353, 2009.

Köhler, H.: The nucleus in and the growth of hygroscopic droplets, Trans. Faraday Soc., 32, 1152–1161, https://doi.org/10.1039/TF9363201152, 1936.

Lowe, S. J.: Modelling the effects of organic aerosol phase partitioning processes on cloud formation, PhD thesis, Stockholm University, Faculty of Science, Department of Environmental Science, Stockholm, Sweden, 2020.

Lowe, S. J., Partridge, D. G., Davies, J. F., Wilson, K. R., Topping, D., and Riipinen, I.: Key drivers of cloud response to surface-active organics, Nat Commun, 10, 5214, https://doi.org/10.1038/s41467-019-12982-0, 2019.

Luoma, K.: AEROSOL OPTICAL PROPERTIES, BLACK CARBON AND THEIR SPATIO-TEMPORAL VARIATION, PhD thesis, University of Helsinki, 2021.

Lutz, A., Mohr, C., Le Breton, M., Lopez-Hilfiker, F. D., Priestley, M., Thornton, J. A., and Hallquist, M.: Gas to Particle Partitioning of Organic Acids in the Boreal Atmosphere, ACS Earth Space Chem., 3, 1279–1287, https://doi.org/10.1021/acsearthspacechem.9b00041, 2019.

Murphy, B. N., Julin, J., Riipinen, I., and Ekman, A. M. L.: Organic aerosol processing in tropical deep convective clouds: Development of a new model (CRM-ORG) and implications for sources of particle number, Journal of Geophysical Research: Atmospheres, 120, 10,441-10,464, https://doi.org/10.1002/2015JD023551, 2015.

Nieminen, T., Asmi, A., Maso, M. D., Aalto, P. P., Keronen, P., Petäjä, T., Kulmala, M., and Kerminen, V.-M.: Trends in atmospheric new-particle formation: 16 years of observations in a boreal-forest environment, Boreal Environ. Res., 19, 191–214, 2014.

Pankow, J. F., Seinfeld, J. H., Asher, W. E., and Erdakos, G. B.: Modeling the Formation of Secondary Organic Aerosol. 1. Application of Theoretical Principles to Measurements Obtained in the α-Pinene/, β-Pinene/, Sabinene/, Δ3-Carene/, and Cyclohexene/Ozone Systems, Environ. Sci. Technol., 35, 1164–1172, https://doi.org/10.1021/es001321d, 2001.

Paramonov, M., Aalto, P. P., Asmi, A., Prisle, N., Kerminen, V.-M., Kulmala, M., and Petäjä, T.: The analysis of size-segregated cloud condensation nuclei counter (CCNC) data and its implications for cloud

droplet activation, Atmos. Chem. Phys., 13, 10285–10301, https://doi.org/10.5194/acp-13-10285-2013, 2013.

Paramonov, M., Kerminen, V.-M., Gysel, M., Aalto, P. P., Andreae, M. O., Asmi, E., Baltensperger, U., Bougiatioti, A., Brus, D., Frank, G. P., Good, N., Gunthe, S. S., Hao, L., Irwin, M., Jaatinen, A., Jurányi, Z., King, S. M., Kortelainen, A., Kristensson, A., Lihavainen, H., Kulmala, M., Lohmann, U., Martin, S. T., McFiggans, G., Mihalopoulos, N., Nenes, A., O'Dowd, C. D., Ovadnevaite, J., Petäjä, T., Pöschl, U., Roberts, G. C., Rose, D., Svenningsson, B., Swietlicki, E., Weingartner, E., Whitehead, J., Wiedensohler, A., Wittbom, C., and Sierau, B.: A synthesis of cloud condensation nuclei counter (CCNC) measurements within the EUCAARI network, Atmospheric Chemistry and Physics, 15, 12211–12229, https://doi.org/10.5194/acp-15-12211-2015, 2015.

Petäjä, T., O'Connor, E. J., Moisseev, D., Sinclair, V. A., Manninen, A. J., Väänänen, R., Lerber, A. von, Thornton, J. A., Nicoll, K., Petersen, W., Chandrasekar, V., Smith, J. N., Winkler, P. M., Krüger, O., Hakola, H., Timonen, H., Brus, D., Laurila, T., Asmi, E., Riekkola, M.-L., Mona, L., Massoli, P., Engelmann, R., Komppula, M., Wang, J., Kuang, C., Bäck, J., Virtanen, A., Levula, J., Ritsche, M., and Hickmon, N.: BAECC: A Field Campaign to Elucidate the Impact of Biogenic Aerosols on Clouds and Climate, Bulletin of the American Meteorological Society, 97, 1909–1928, https://doi.org/10.1175/BAMS-D-14-00199.1, 2016.

Petters, M. D. and Kreidenweis, S. M.: A single parameter representation of hygroscopic growth and cloud condensation nucleus activity – Part 2: Including solubility, Atmos. Chem. Phys., 7, 2008.

Riipinen, I., Rastak, N., and Pandis, S. N.: Connecting the solubility and CCN activation of complex organic aerosols: a theoretical study using solubility distributions, Atmospheric Chemistry and Physics, 15, 6305–6322, https://doi.org/10.5194/acp-15-6305-2015, 2015.

Roelofs, G. J. H.: Drop size dependent sulfate distribution in a growing cloud, J Atmos Chem, 14, 109–118, https://doi.org/10.1007/BF00115227, 1992.

Ruehl, C. R., Chuang, P. Y., Nenes, A., Cappa, C. D., Kolesar, K. R., and Goldstein, A. H.: Strong evidence of surface tension reduction in microscopic aqueous droplets, Geophysical Research Letters, 39, https://doi.org/10.1029/2012GL053706, 2012.

Ruehl, C. R., Davies, J. F., and Wilson, K. R.: An interfacial mechanism for cloud droplet formation on organic aerosols, Science, 351, 1447–1450, https://doi.org/10.1126/science.aad4889, 2016.

Schmale, J., Henning, S., Decesari, S., Henzing, B., Keskinen, H., Sellegri, K., Ovadnevaite, J., Pöhlker, M. L., Brito, J., Bougiatioti, A., Kristensson, A., Kalivitis, N., Stavroulas, I., Carbone, S., Jefferson, A., Park, M., Schlag, P., Iwamoto, Y., Aalto, P., Äijälä, M., Bukowiecki, N., Ehn, M., Frank, G., Fröhlich, R., Frumau, A., Herrmann, E., Herrmann, H., Holzinger, R., Kos, G., Kulmala, M., Mihalopoulos, N., Nenes, A., O'Dowd, C., Petäjä, T., Picard, D., Pöhlker, C., Pöschl, U., Poulain, L., Prévôt, A. S. H., Swietlicki, E., Andreae, M. O., Artaxo, P., Wiedensohler, A., Ogren, J., Matsuki, A., Yum, S. S., Stratmann, F., Baltensperger, U., and Gysel, M.: Long-term cloud condensation nuclei number concentration, particle number size distribution and chemical composition measurements at regionally representative observatories, Atmospheric Chemistry and Physics, 18, 2853–2881, https://doi.org/10.5194/acp-18-2853-2018, 2018.

Shrivastava, M., Cappa, C. D., Fan, J., Goldstein, A. H., Guenther, A. B., Jimenez, J. L., Kuang, C., Laskin, A., Martin, S. T., Ng, N. L., Petaja, T., Pierce, J. R., Rasch, P. J., Roldin, P., Seinfeld, J. H., Shilling, J., Smith, J. N., Thornton, J. A., Volkamer, R., Wang, J., Worsnop, D. R., Zaveri, R. A., Zelenyuk, A., and Zhang, Q.: Recent advances in understanding secondary organic aerosol: Implications for global climate forcing, Reviews of Geophysics, 55, 509–559, https://doi.org/10.1002/2016RG000540, 2017.

Sihto, S.-L., Mikkilä, J., Vanhanen, J., Ehn, M., Liao, L., Lehtipalo, K., Aalto, P. P., Duplissy, J., Petäjä, T., Kerminen, V.-M., Boy, M., and Kulmala, M.: Seasonal variation of CCN concentrations and aerosol activation properties in boreal forest, Atmospheric Chemistry and Physics, 11, 13269–13285, https://doi.org/10.5194/acp-11-13269-2011, 2011.

Topping, D., Connolly, P., and McFiggans, G.: Cloud droplet number enhanced by co-condensation of organic vapours, Nature Geosci, 6, 443–446, https://doi.org/10.1038/ngeo1809, 2013.

Topping, D. O. and McFiggans, G.: Tight coupling of particle size, number and composition in atmospheric cloud droplet activation, Atmospheric Chemistry and Physics, 12, 3253–3260, https://doi.org/10.5194/acp-12-3253-2012, 2012.

Wang, Y., Chen, Y., Wu, Z., Shang, D., Bian, Y., Du, Z., Schmitt, S. H., Su, R., Gkatzelis, G. I., Schlag, P., Hohaus, T., Voliotis, A., Lu, K., Zeng, L., Zhao, C., Alfarra, M. R., McFiggans, G., Wiedensohler, A., Kiendler-Scharr, A., Zhang, Y., and Hu, M.: Mutual promotion between aerosol particle liquid water and particulate nitrate enhancement leads to severe nitrate-dominated particulate matter pollution and low visibility, Atmospheric Chemistry and Physics, 20, 2161–2175, https://doi.org/10.5194/acp-20-2161-2020, 2020.

Yatavelli, R. L. N., Mohr, C., Stark, H., Day, D. A., Thompson, S. L., Lopez-Hilfiker, F. D., Campuzano-Jost, P., Palm, B. B., Vogel, A. L., Hoffmann, T., Heikkinen, L., Äijälä, M., Ng, N. L., Kimmel, J. R., Canagaratna, M. R., Ehn, M., Junninen, H., Cubison, M. J., Petäjä, T., Kulmala, M., Jayne, J. T., Worsnop, D. R., and Jimenez, J. L.: Estimating the contribution of organic acids to northern hemispheric continental organic aerosol, Geophysical Research Letters, 42, 6084–6090, https://doi.org/10.1002/2015GL064650, 2015.

Ylivinkka, I., Kaupinmäki, S., Virman, M., Peltola, M., Taipale, D., Petäjä, T., Kerminen, V.-M., Kulmala, M., and Ezhova, E.: Clouds over Hyytiälä, Finland: an algorithm to classify clouds based on solar radiation and cloud base height measurements, Atmospheric Measurement Techniques, 13, 5595–5619, https://doi.org/10.5194/amt-13-5595-2020, 2020.